DESIGN AND OPTIMIZATION OF SHAFT BRACKET OF DRUM BRAKE FOR HEAVY DUTY VEHICLE

A Thesis Submitted to
the Graduate School of Engineering and Sciences of
İzmir Institute of Technology
in Partial Fulfillment of the Requirements for the Degree of

MASTER OF SCIENCE

In Mechanical Engineering

by
Mert ÇETİN

July 2021
İZMİR

To My Family…

ACKNOWLEDGMENTS

I would like to express my endless thanks to my academic supervisor Prof. Dr. H. Seçil ARTEM for her continuous support, patience, motivation, and valuable advice. I will always be proud to work with Prof. Artem throughout my thesis study.

Besides my supervisor, I would like to express my thanks to my colleagues, Barış YILMAZ, who guided me at every stage with their valuable ideas and opinions; Bora GÜNTAY for their assistance in the realization of the test processes; İ.Can GÜLERYÜZ for their assistance in the studies of computer-aided engineering and EGE FREN A.Ş. which provided the software and test equipment needed to realize the project and allowed its use.

Furthermore, I offer sincere thanks to my family who has always encouraged me along this way.

Lastly, I would like to thank the people who helped me directly and indirectly.

ABSTRACT

DESIGN AND OPTIMIZATION OF SHAFT BRACKET OF DRUM BRAKE FOR HEAVY DUTY VEHICLE

The automotive industry is one of the leading sectors with a wider market share than any other sector which can quickly adapt to the increasingly competitive environment. However, in addition to the increasing product costs, regulations aiming to reduce fuel consumption and carbon emissions require an optimal design that satisfies design requirements depending on seriously increasing competition in this sector. This situation aims to design lightweight and high-performance vehicle products in a shorter period. In this sense, optimization methods have become very popular especially with the development of computer technologies in recent years. Therefore, they are often preferred in the design of vehicle products which enable to achieve the most suitable design for the specified purpose in a short time.

This thesis study aims to realize a new shaft bracket design to be used in Z-Cam drum brakes of heavy duty vehicles by optimization methods. In line with this goal, firstly, the boundaries of material distribution in the given design space for vehicle axle application were obtained with the help of topology optimization. Then shape optimization was applied to bring material distribution having the suitable rough surfaces into the manufacturable form. Here, the Solid Isotropic Microstructure with Penalization (SIMP) algorithm was used for topology optimization and Response Surface Method (RSM) for shape optimization. Finite element analysis (FEA) of the final design obtained due to optimization was repeated and design verification tests were performed on the shaft bracket prototype manufactured according to the final design. The effectiveness and applicability of the optimization method used in the study were examined by comparing the performed test results with the final FEA. As a result of this study, a lighter design having a 72% weight advantage was obtained instead of the existing shaft bracket and the new design showed the similar structural strength compared with the existing shaft bracket as a result of experimental verification tests. Consequently, it has been seen that the optimization methods are very effective for the structural design of vehicle products.

Keywords: *Topology Optimization, Shape Optimization, Finite Element Analysis, Computer Aided Engineering, Z-cam Drum Brake, Heavy Duty Vehicles.*

ÖZET

AĞIR HİZMET ARAÇLARI İÇİN KAMPANALI FREN MİL BRAKETİ TASARIMI VE OPTİMİZASYONU

Otomotiv sanayisi diğer sektörlere kıyasla daha geniş pazar payına sahip ve artan rekabet ortamına çabuk uyum sağlayan öncü sektörlerden biridir. Ancak son yıllarda artan ürün maliyetleri ile birlikte, yakıt tüketimi ve karbon salınımı azaltılmasına yönelik düzenlemeler, bu sektördeki rekabeti arttırarak tasarım hedeflerini karşılayan optimum ürünlerin ortaya konmasını gerektirmektedir. Bu durum, daha kısa zaman zarfında, daha hafif ve daha yüksek performanslı ürünlerin tasarlanmasını hedeflemektedir. Bu bağlamda, özellikle son yıllarda teknolojik ürünlerin gelişimi ile oldukça popüler hale gelmiş olan ve daha kısa sürede belirlenmiş amaca en uygun tasarım elde etmeyi sağlayan optimizasyon yöntemleri, otomotiv parçaları tasarımında sıklıkla tercih edilmektedir.

Bu tez çalışmasında, ağır hizmet araçlarının Z-kamlı kampanalı frenlerinde kullanılacak olan yeni mil braketi tasarımının optimizasyon yöntemleri ile gerçekleştirilmesi hedeflenmiştir. Bu hedef doğrultusunda, araç dingil platformuna uygun tasarımın genel hatları, topoloji optimizasyonu ile elde edilmiş, elde edilen yapının üretilebilir forma getirilebilmesi için şekil optimizasyonu uygulanmıştır. Burada, topoloji optimizasyonu için Cezalandırma Faktörü İle Katı İzotropik Mikro Yapılar (SIMP) algoritması, şekil optimizasyonu için ise Cevap Yüzeyi Yöntemi (RSM) kullanılmıştır. Optimizasyon sonucu elde edilen final tasarımın sonlu elemanlar analizleri tekrarlanmış ve final tasarıma göre üretilen mil braketi numunesi üzerinde tasarım doğrulama testleri gerçekleştirilmiştir. Elde edilen test sonuçları ile optimizasyon sonrası sonlu elemanlar analizi sonuçları kıyaslanarak gerçekleştirilen çalışmada kullanılan optimizasyon yönteminin etkinliği ve uygulanabilirliği incelenmiştir. Gerçekleştirilen çalışma sonucunda, mevcut mil braketi yerine %72 daha hafif bir yapı elde edilmiş ve gerçekleştirilen deneysel doğrulama testleri ile yeni tasarımın, mevcut tasarım ile benzer dayanım gösterdiği ortaya konmuştur. Tüm bunlar neticesinde, optimizasyon yönteminin yapı tasarımındaki ihtiyaçları karşılanması açısından oldukça etkili olduğu açıkça görülmüştür.

Anahtar Kelimeler: *Topoloji Optimizasyonu, Şekil Optimizasyonu, Sonlu Elemanlar Analizi, Bilgisayar Destekli Mühendislik, Z-kam Kampanalı Fren, Ağır Hizmet Araçları.*

TABLE OF CONTENTS

LIST OF FIGURES

Figure **Page**

Figure **Page**

LIST OF TABLES

Table **Page**

CHAPTER 1

INTRODUCTION

1.1. Literature Survey

In recent years, the design of cost-effective and high-performance vehicle products has been one of the challenging issues in the automotive industry. Particularly, in addition to increasing manufacturing and engineering costs, regulations to reduce carbon emission and fuel consumption require lightweight and environmentally friendly vehicle products that meet design targets by increasing competition in this sector directly (Sudin, et al. 2014).

The structural design of vehicle products is regarded as one of the most significant tasks for automotive engineering studies. Because, this process highly depends on the designer's experience, creativity, and intuition. Traditionally, the structural design is achieved through a trial-and-error approach iteratively. However, limited material resources, technological competition, and environmental impact make this process very time-consuming and costly. Furthermore, this design process sometimes causes the optimal solution to be ignored because it is based on intuitive thinking. Unlike traditional and experience-based methods, new techniques are needed that can give more efficient results (Yıldız, et al. 2004). Therefore, structural optimization methods play an important role to propose an optimal design in the structural design process of vehicle products without sacrificing their performance (Sudin, et al. 2014).

Optimization can be defined as finding the best or optimal design that satisfies all the constraints under specified single or multi objectives. In the structural design process, optimization is regarded as designing the highest quality structure, which means that all design requirements are met with minimal resources.

One of the most used structural optimization methods in structural design process is topology optimization. It is a well-known and powerful method to pursuing a lightweight and high-performance structure without losing its best performance. The most important reason for topology optimization preferred by designers is that the optimal

design is revealed at the beginning stage of the design process without having detailed knowledge (Albak 2019). With the help of this method, it is possible to obtain an optimal design in a shorter time and related design engineering costs are minimized in the product design process.

Recently, with progress in computer science and technology, structural designs by optimization methods have become the focus of attention of researchers in the automotive industry to obtain lightweight and high-performance structures (Liu, et al. 2018). In this sense, various structural design studies for axle and wheel-end components have been carried out in the literature using optimization methods.

Mathur and Kurna (2015) studied the weight optimization of existing axle beam by reducing unsprung mass for cost-saving and ride comfort improvement of the vehicle. For this study, an I-section beam connecting the knuckle and wheel-end components was taken due to the having importance in terms of weight of unsprung mass and the various beam section parameters such as width, horizontal and vertical flange height were determined depending on manufacturing constraints for shape optimization method. Under severe braking and road conditions, the study was conducted by using OptiStruct software and as a result of the study, a weight advantage of about 9 kg was provided for the existing axle beam with 50 kg.

Topac and Atak (2016) studied the design and optimization process of an axle beam used in heavy duty commercial vehicles. For the created parametric axle body model having an I-section shape, Design of Experiment (DOE)-based shape optimization was conducted to improve both weight and stress concentration with the help of ANSYS Workbench software. According to the two selected parameters, nine experimental design points were created by using central composite design, and response surfaces were obtained to equivalent stress and axle mass. As a result of this study, the maximum stress values on the critical section of axle beam were reduced to 25% and axle beam weight was optimized about 10% in comparison with the commercial axle beams that are used in the local market within the same loading capacity.

Zhang et al. (2019) studied the optimization of a brake shoe of the drum brake. Based on the results of static and modal analysis, the topology optimization was carried out with the help of ANSYS software. It was concluded that the maximum stress after optimization was 335 MPa same as the before optimization and the natural frequency of the brake shoes was improved. As a result of the study, the feasibility of the optimization method was verified which provides an idea for the design of vehicle products.

Nagatani and Niwa (2005) studied topology and shape optimization for the development of hub-bearing lightening in terms of fuel efficiency. In this study, the homogenization-based topology optimization method was conducted to obtain optimal structure and distortion energy minimization was set as objective with respect to the 22.5%, 27.5%, and 30% relative. Then, volume minimization respected to the principal stress as below the current level was conducted with shape optimization to determine the optimum dimensions. As a result of the study, a weight reduction was provided with this methodology and the target mass of 1.0 kg was achieved. However, this newly developed hub bearing was found to be unsuitable for drum brake structures where the hub bearing also functioned as a brake seal.

Yıldız et al. (2004) studied an optimal design of the engine mount bracket under dynamic loading conditions. The research was presented to create an initial design concept in terms of optimal structural layout by using optimization approaches. In line with this purpose, the topology optimization was conducted for the concept design phase and then, the shape optimization was subsequently employed to determine an optimal design satisfying all specified requirements with minimum factors by using initial optimal topology. Here, for topology optimization, the objective function was chosen to minimize the compliance and to maximize the natural frequency with respect to the 75% material usage imposed constraint. For shape optimization, the objective was defined to minimize the mass of the engine mount bracket with respect to the maximum stress constraint. As a result of the study, although it was seen that optimization methods could lead to obtain acceptable results, experimental results were needed to verify the effectiveness of the used methods.

Sergent et al. (2014) studied a topology optimization approach for optimal design of a four-piston caliper for disc brake assembly. By the using computer-based topology optimization method in Altair Optistruct software, two different optimized caliper designs were obtained depending on two different load cases. With the specified optimization objective as volume minimization for minimum mass under different load cases, both designs offered a considerable reduction of caliper mass, by 19% and 28%, respectively.

Güleryüz and Yılmaz (2019) were performed an optimization study to reduce the unsprung mass of the vehicle by using computer-aided engineering (CAE) tool. With the help of topology optimization by using ANSYS software, weight reduction of existing torque plate of Z-cam drum brake was investigated. The aim was to optimize the torque plate for minimum mass under given stiffness. Thus, the optimization objective was

minimizing the torque plate weight by 30%. As a result of the study, it is observed that a significant decrease in stress level accompanied by a considerable reduction in casting and machined torque plate masses by 11.9% and 12.2%, respectively.

Sudin et al. (2014) studied a topology optimization approach to reduce the weight of an existing brake pedal design of a car. For a new lightweight design brake pedal, the objective function was determined as mass minimization while maintaining its integrity under certain design constraints. Hereby, the design constraints that give minimum safety factor 1.5 were defined as the maximum equivalent stress must be below yield strength and maximum acceptable total deformation cannot exceed 10 mm. As a result of the topology optimization by using Altair Optistruct software, the weight of the newly designed brake pedal was reduced by 22% as compared to an existing brake pedal without sacrificing its performance requirement.

Enginar (2014) studied the optimal design of a heavy vehicle wheel using optimization methods in Altair HyperWorks software. Firstly, a parametric shape optimization study was carried out to make the air hole form, where the maximum stress was seen, dependent on a single design parameter. Thus, the maximum stress value was reduced from 398.8 MPa to 370 MPa without changing the model weight. Afterward, a topology optimization study was carried out to achieve weight advantage from disc form. Here, compliance minimization was set as an objective function of topology optimization and 75% volume fraction was defined as constraint function. As a result of the study, in the model, which stands out as the first candidate among the acceptable solutions, the maximum stress value increased to 371.6 MPa even though the weight decreased to 16.75 kg. In the second solution model, 23 MPa reduction in stress and 0.46 kg lightening in weight were achieved when compared to the stress and weight values of the reference wheel.

Işık (2009) studied to implement structural topology optimization methods on driveshaft part called flange yoke, which maintains the connection of a driveshaft between gearbox output and differential input flanges in Altair Optistruct software. Here, mass minimization was defined as an objective function and the constraint was defined so that the maximum amount of deformation did not exceed 0.135 mm for topology optimization. After completing topology optimization activities, a new geometry was derived from the optimized topology. FEA methods and experimental tests were used to compare and verify the stress distribution and total displacement of the new geometry with the existing ones. According to the results, positive results were obtained and it was predicted that the

optimum geometry designed with the help of topology optimization would show similar performance compared with the existing products. As a result of the topological optimization study, the weight of the flange yoke was reduced by 12%.

Düzcan (2019) studied the development of vehicle suspension components with structural optimization techniques in Altair Optistruct software. First, static analysis was performed to evaluate the state of the existing structure, and then material distribution is obtained with the help of topology optimization. Afterward, it was aimed to reduce stress values in local areas with shape optimization applied after topology optimization process. As a result of the study, optimum and structurally improved design has been achieved by using topology and shape optimization in the suspension cover used in suspension systems and the weight of the optimum design was reduced by 35.2%, and the maximum stress decreased by 8.3% compared to the existing design.

Topac et al. (2020) carried out a numerical case study to perform the lightweight design of a connection bracket, which is used in the rear axle of an articulated truck. By using a composite method including a finite element (FE) based topology optimization and response surface methodology (RSM) based optimization were employed. Here, strain energy minimization subjected to the volume constraint is used to obtain the stiffest design for the connection bracket was specified with topology optimization. According to the topology result, the bracket was redesigned and FEA was conducted to determine the stress locations. In order to eliminate or reduce the critical stress values, the RSM-based optimization was performed. As a result of the study, numerical results indicated that by using topology optimization, it was possible to reduce the mass of the bracket by about 63% in comparison with the original design and the equivalent stress at the most critical regions of the component was decreased up to 62%.

Tyflopoulos and Steinert (2020) conducted topology and parametric optimization for the identification of the ideal material optimization procedure based on the design process of the lightweight structure. The main reason of this study is to propose which optimization procedure can lead to the best results based on material reduction and optimization time in the literature. According to the study, a quantitative comparison of different topology and parametric optimization design processes were conducted using three benchmark examples and ten different design processes that were developed in each case study resulted in 30 simulations in total. In addition to this, their results were compared with respect to mass, stress, and time. As a result of study, the simultaneous

parametric and topology optimization approach gave the lightest design solutions without compromising their initial strength but also increased the optimization time.

1.2. Objectives of the Study

According to the literature review, it is clearly seen that there is anemphasis on structural design studies for lightweight and cost-effective vehicle components. Therefore, the structural optimization methods by using computer aided techniques play an important role to lead achieving optimal design.

The shaft bracket which is one of key component of the Z-cam drum brake shown in Figure 1.1 is fitted to the torque plate directly. This structure built up with sheet metal components by using welded manufacturing method provides the transfer of the braking force created by the brake chamber to the shoes by helping the mounting of the brake chamber on the relevant surface. Furthermore, it helps the camshaft to hold in the bracket tube with bushing. Since it plays an important role during braking, it is desired to transfer the air chamber force to both shoes efficiently within the targeted cycle period. However, design-related problems affect braking negatively during its operation and these situations cause loss of braking performance directly.

Figure 1.1. Shaft bracket of Z-cam drum brake
(Source: Ege Fren 2021)

In some vehicle axle applications, it is not possible to fit the shaft bracket to the torque plate directly due to the lack of sufficient volume. Moreover, an increase in the length of the shaft bracket structure including the camshaft causes weight increase in terms of the brake assembly as well. So instead, it is proposed a new shaft bracket design which is to be assembled on the vehicle axle directly. At this moment, this new design should be as light and competitive as possible to minimize fuel consumption and carbon emissions without causing loss of brake performance during braking, taking into account the working conditions of the camshaft. For that reason, an optimal design must be realized that meets these design targets.

In this thesis study, structural optimization methods were employed to design the optimal structure instead of the existing shaft bracket used in the Z-cam drum brakes of heavy duty vehicles shown in Figure 1.1. The contributions of this study were summarized as follows:

(1) To introduce optimal design which is lighter, high efficient, and cost-effective that meets the design requirement instead of the existing shaft bracket for suitable axle platform of the heavy duty vehicle.

(2) To conduct topology optimization to obtain rough material distribution with mass minimization with respect to the stress constraint instead of compliance minimization, widely used in the literature and Optimal Space Filling Design (OSFD) for shape optimization.

(3) To construct structural design methodology by using modern computer technologies and investigate the capabilities of optimization methods in terms of how a better structural design can be achieved within shorter design process and limited conditions.

The flowchart of the work done in this thesis is given in Figure 1.2.

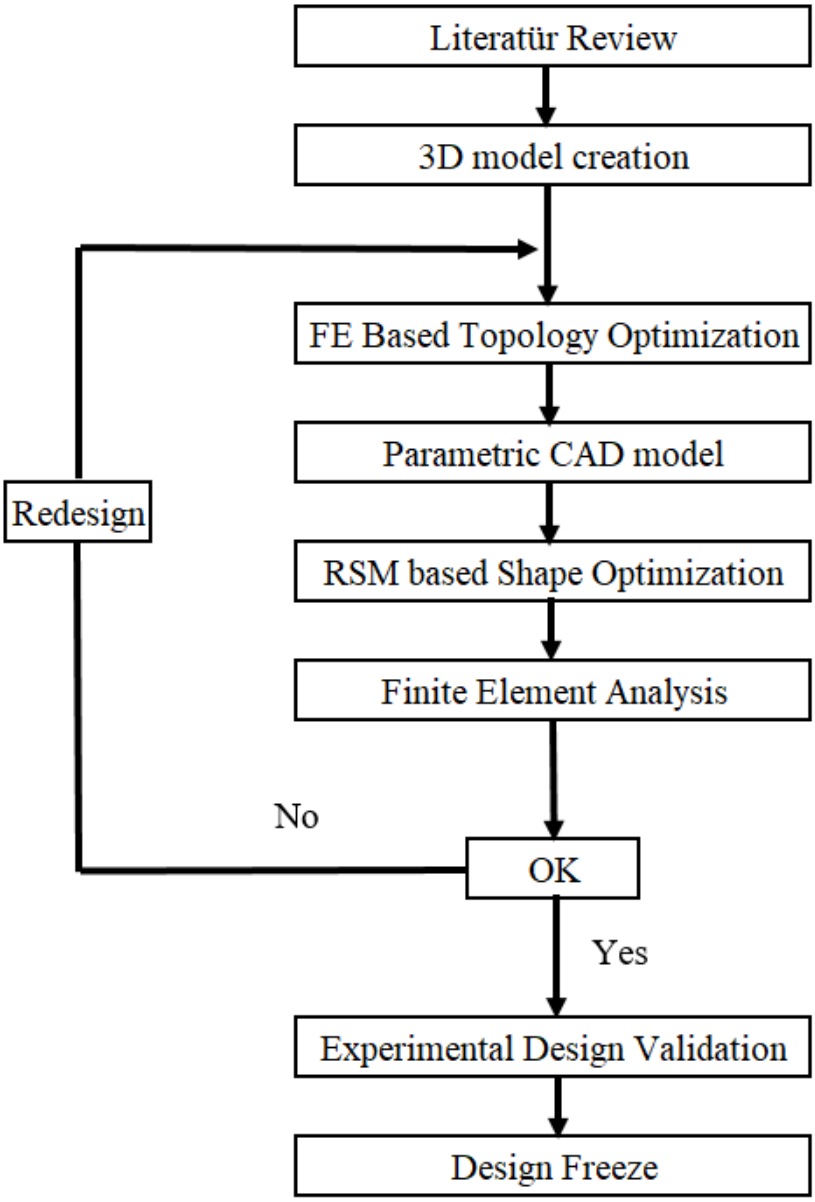

Figure 1.2. Flowchart for structural desing process

CHAPTER 2

THEORETICAL BACKGROUND

2.1. Brake System

Brake system is one of the most important components of a vehicle. The brake system designed to slow or stop the moving vehicle keeping the vehicle speed constant on downhill roads or to hold a vehicle stationary on a grade by providing the control and safety of the vehicle (Limpert 2011). The main function of the brake system is to convert the kinetic energy of the vehicle into heat and braking energy through friction by transferring the force applied by the driver on the brake pedal to the friction elements on the vehicle via a brake actuator system (Ghazaly and Makrahy 2014).

For the road vehicles, the friction based brakes shown in Figure 2.1 are classified into disc brake and drum brake.

(a) (b)

Figure 2.1. Types of brakes: (a) disc brake, (b) drum brake
(Source: Ege Fren 2021)

Disc brakes include friction materials and a rotor that has friction surfaces. This rotor rotates with the wheel together while in motion. The friction materials named pads are pressed against each side of the rotating rotor with a force generated by air pressure and this motion generates the friction forces needed for the braking. Drum brakes,

consisting of drum and brake mechanism, use internal expanding shoes driven by a cam mechanism. Thereby, braking is generated by pressing these shoes against the rotating drum. The main advantage of drum brakes provide more stopping power compared to disc brakes, for a given amount of force applied to the brake pedal (Mahmoud 2005).

Drum brakes are the first type of brake systems used in the automotive industry for many years and drum brake types such as S-cam, Z-cam, and wedge drum brakes are still widely preferred in North America and the rest of the world in Europe for heavy commercial vehicle applications (Güleryüz and Yılmaz 2019). Although the disc brakes are preferred brakes in some vehicle types compared with the drum in recent years, the drum brakes still can be seen at the rear wheel of the passenger cars and all wheels of commercial vehicles. The reason for this situation in addition to generating more braking power, the drum brakes have lower production costs and provide easy maintenance opportunities due to their simple design (Baba, et al. 2018).

2.2. Z-Cam Drum Brake

Z-cam drum brake is one of the drum brake types widely used in heavy duty vehicle applications. Assembly and exploded views of the Z-cam drum brake are shown in Figure 2.2.

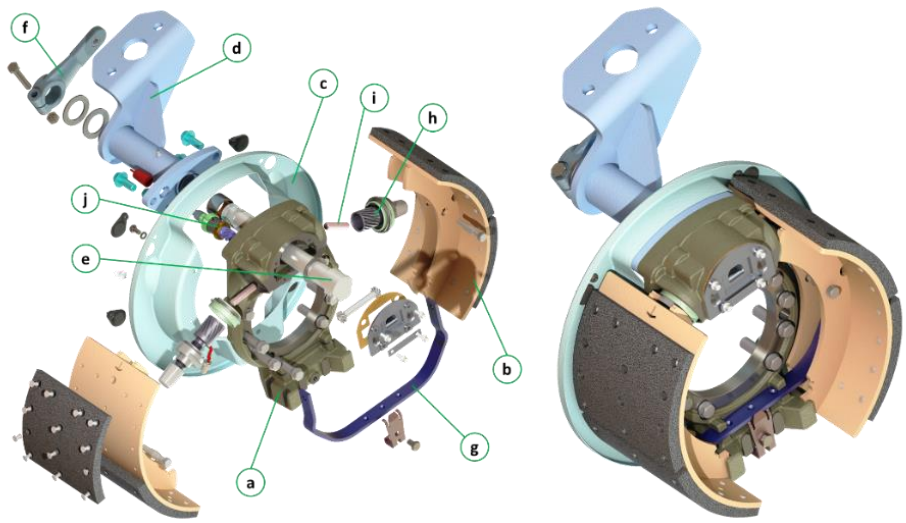

Figure 2.2. Z-cam drum brake components: (a) torque plate, (b) leading and trailing shoes, (c) dust shield, (d) shaft bracket, (e) camshaft, (f) lever, (g) C-spring, (h) tappet heads, (i) struts and (j) parts of automatic adjustment mechanism
(Source: Güleryüz and Yılmaz 2019)

The Z-cam drum brake mainly consists of two braking shoes, torque plate, shaft bracket, and subassembly parts. The Z-cam drum brake is assembled on the vehicle's axle flange or steering knuckle by fixation bolts.

2.3. Working Principle of Z-Cam Drum Brake

In Z-cam brake, braking starts from the air brake chamber. When the driver presses the brake pedal, high air pressure stored in the air tank enters into the air brake chamber and applies a force on the rubber diaphragm in the air brake chamber. This force allows movement of the diaphragm and the pushrod located on the diaphragm to move outward direction. As a result, braking is achieved by converting air pressure into mechanical force (Awate, et al. 2016).

The air brake chamber comprising return spring, diaphragm, pushrod, air inlet, and outlet connections is shown in Figure 2.3.

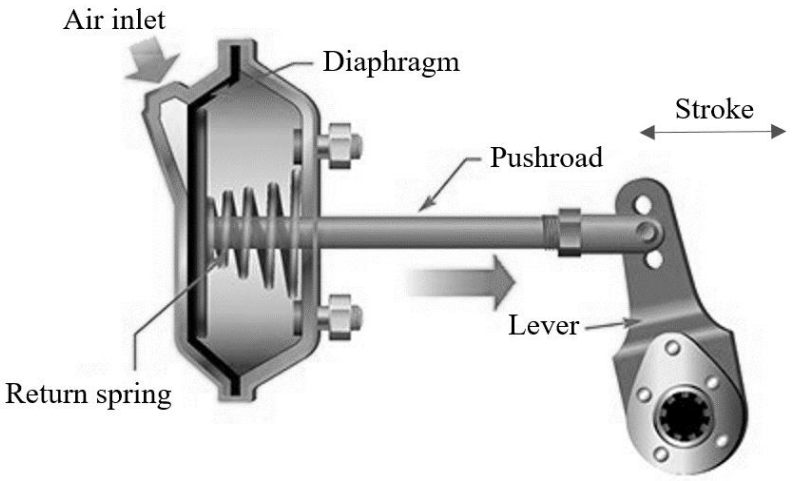

Figure 2.3. Air brake chamber
(Source: https://www.ontario.ca/document/official-air-brake-handbook/service-brake-subsystem)

After the air brake chamber generates a mechanical force, this force creates a rotary motion on the lever. And then, this force is transmitted to the brake shoes from the Z-camshaft, thrust heads, and struts, respectively. Shoes slide along their abutments at one

end, while they are mechanically actuated by tappet heads at another end. In case of braking, a gap is occured between the linings and the drum due to wear of the brake pads. This gap is compensated by using an automatic adjustment mechanism over time (Kuralay 2008).

In case of braking, pushrod stroke is a critical indicator in terms of the performance of an air brake system. As the pushrod strokes out of the air brake chamber, it rotates the lever by the same angle. This situation increases the contact of the brake shoes to the drum by moving out the struds on the camshaft in case of braking and generates higher braking force. However, this situation cannot be realized as described. As the pushrod stroke increases, the braking force generated by the brake chamber changes depending on its design characteristic and elastically deformation is occurred on the shaft bracket due to the change of forces acting on the shaft bracket. This situation directly affects the brake efficiency by causing a change in the braking force to be produced. The change of air chamber force depending on the pushrod stroke according to the DIN 74060-1 standard is illustrated in Figure 2.4.

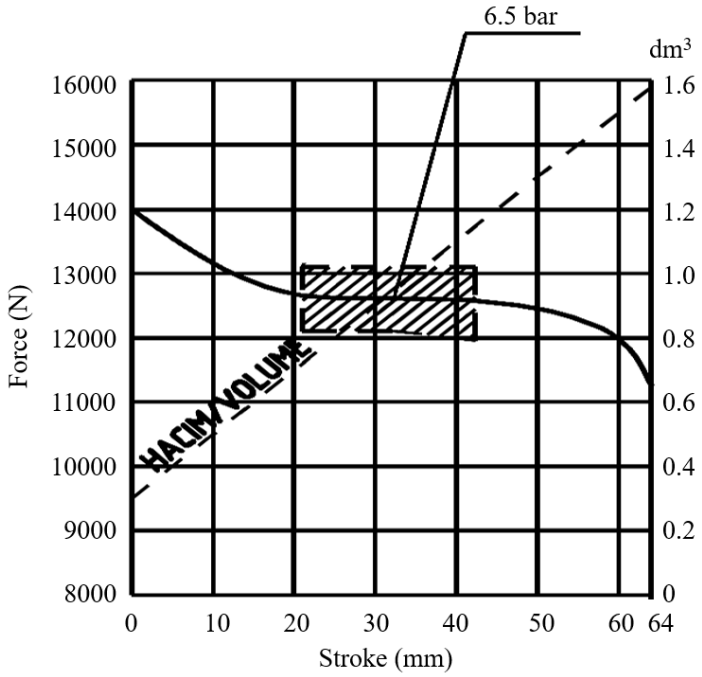

Figure 2.4. Stroke and force diagram of Type30 air chamber
(Source: DIN 74060-1)

CHAPTER 3

OPTIMIZATION

Optimization is widely used in many different industrial fields such as aerospace, automobile, biomedicine, etc. Engineers always tend to find suitable solutions that provide the highest quality and satisfy design requirements with limited resources. However, these solutions cannot be easily achieved. In this sense, optimization methods have emerged in recent years as popular and powerful methods for solving complex engineering optimization problems.

Optimization is the act of obtaining the best result under given circumstances to identify the best candidate from a collection of alternatives. The main purpose of the optimization is either to minimize the effort required or to maximize the desired benefit. Since the effort required or the benefit desired in any practical situation can be expressed as a function of certain decision variables, optimization can be defined as the process of finding the conditions that give the maximum or minimum value of a function (Rao 2019).

The design of lightweight and cost-effective vehicle products is one of the essential issues in the automotive industry. In addition to the decreasing material resources and increasing raw material costs affecting the product costs, strategies to improve fuel consumption and comply with carbon emission regulations require more efficient structural designs making the most significant problems of the sectoral competition. However, the critical problem in structural design is how to achieve an optimal design at the beginning of the design process. Because the classic trial-and-error approach requires various iterations to design products, this process is highly time-consuming and cannot represent the best design solution. This situation has forced engineers to find decision-making methods such as optimization to design both economically and efficiently solutions. Hence, to overcome these deficiencies, structural optimization methods have been employed to determine the optimal product design in terms of lightweight and cost-effective vehicle products by yet satisfying the stiffness and dynamic performance requirements of a component (Yaban 2012).

3.1. Statement of an Optimization Problem

In a structural design problem, there is no single acceptable design solution and the main purpose of optimization is to choose an optimal or an acceptable one among the design solutions by comparing it with a created mathematical model (Rao 2019).

The fundamental structural design problem can be described by the objective of the problem, a set of design variables, and the design constraints. For that reason, the structural optimization problem can be formulated as minimizing the objective function concerning the constraints. Design variables regarded as optimization variables affect the performance of the analyzed structure by being treated during the optimization process to achieve the purpose of the problem. Design constraints represent the boundaries of design variables meaning physical limitations of fabricability. In order to define a design optimization problem, a minimum number of design variables are required that should be independent of each other as far as possible. A numerical value should be given to each identified design variable to determine if a trial design of the system is specified (Arora 2004).

The optimization problem defined with mathematical formulation includes objective functions, design constraints, and design variables. The mathematical formulation is used in optimization modeling to relate how the decision variables affect the state variables of the optimization problem. Here, the objective function is used to decide on the most suitable one by comparing the different acceptable solutions of the optimization process, while design variables include state variables of the optimization problem (Willis and Finney 2012).

An optimization problem can be expressed mathematically as follows (Rao, 2019):

$$\text{Find } X = \begin{cases} x_1 \\ x_2 \\ \cdot \\ \cdot \\ x_n \end{cases} \text{ which minimizes or maximizes } F(X) \qquad (3.1)$$

Subject to constraints

$$g_j(X) \leq 0 \quad , \quad j = 1, 2, \ldots, m \tag{3.2}$$

$$h_j(X) = 0 \quad , \quad j = 1, 2, \ldots, p \tag{3.3}$$

where X is an *n*-dimensional design vector that includes the n number of design variables, $X=\{x_1, x_2, \ldots, x_n\}^T$, and F($X$) is the objective function. $g_j(X)$ and $h_j(X)$ are known as m number inequality and p number equality constraints, respectively.

The illustration of the optimization problem is shown in Figure 3.1. It can be seen from the figure that point x* corresponds to the minimum value of function F(X) and the maximum value of the negative of the function, -F(X) at the same time. This means that optimization can be regarded as minimization while the maximum of a function can be found by searching for the minimum of the negative of the same function without loss of generality (Rao 2019)

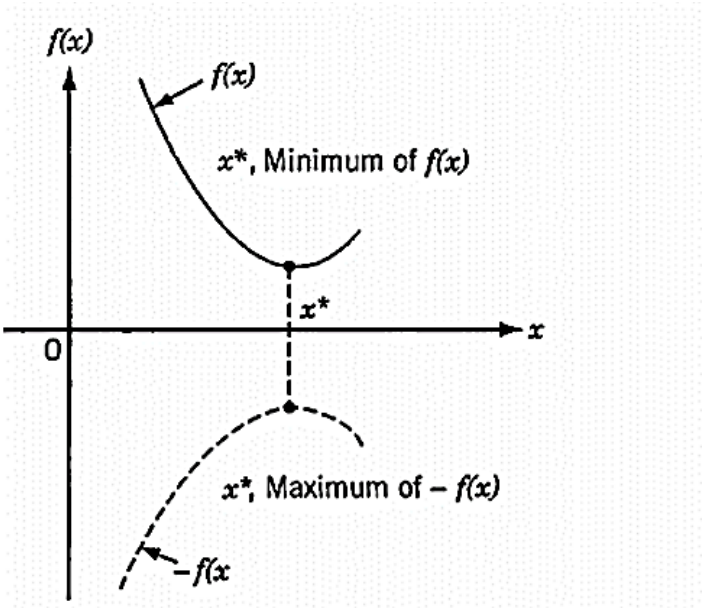

Figure 3.1. Optimization diagram
(Source: Rao 2019)

3.2. Types of Structural Optimization

Structural optimization is regarded as a systematic methodology to increase the structural performance of components and mechanical systems (Sant'Anna and Fonseca 2002). Structural optimization is a useful product design method concerned with maximizing the utility of limited resources to fulfill a given objective. Structural optimization finds the design that performs best against various design constraints in a given material layout. Optimal structural design is becoming highly essential due to the limited material resources, environmental impact, and technological competition, all of which demand lightweight, low-cost and high-performance structures (Thummar 2014). There are many structural optimization methods, each with its own advantages and disadvantages. The structural optimization types can roughly be divided into three parts: size, shape, and topology optimization.

3.2.1. Size Optimization

Size optimization is the easiest and earliest method to improve structural performance and it can be seen as a simplified type of topology optimization (Olason and Tidman 2010). The shape of the design is kept as fixed throughout the optimization process and it is aimed to find the optimum dimensions of design parameters defined on the geometry such as cross-sectional area, material thickness, etc., changing within predetermined structural limits (Abdi 2015). A two-dimensional size optimization depending on design parameters is seen in Figure 3.2.

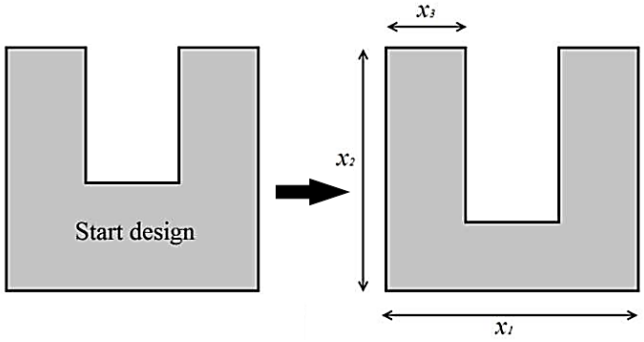

Figure 3.2. Size optimization
(Source: Abdi 2015)

3.2.2. Shape Optimization

Shape optimization in a general setting requires the determination of the optimal spatial material distribution for given loads and boundary conditions (Bendsøe 1989). After the material distribution are revealed via topology optimization, it is necessary to determine the final dimensions. In shape optimization, the shape of the boundaries changes during the optimization process by keeping constant the topology of the geometry (Abdi 2015). A two-dimensional shape optimization is seen in Figure 3.3.

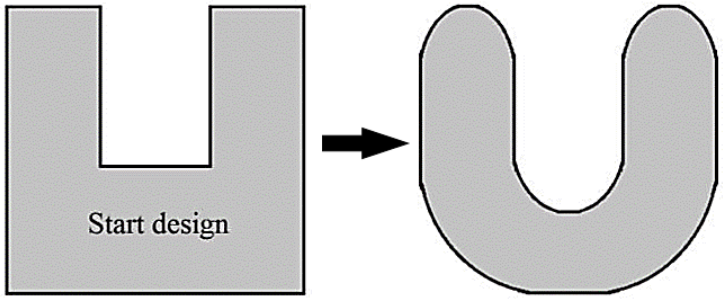

Figure 3.3. Shape optimization
(Source: Abdi 2015)

Shape optimization is used to fine-tune for a chosen design topology in terms of performance and manufacturability, while topology optimization is used to produce concept designs. A main difference among the optimization methods is that the design variables in shape optimization each affect many elements instead of having one or more design variables for each element (Olason and Tidman 2010).

3.2.3. Topology Optimization

Topology derived from Greek words topos (meaning surface or space) and logos(meaning science) is explained as one of the main disciplines of mathematics in which geometric features and dimensional relationships are not affected by the continuous change of parts, shapes and sizes. Topology optimization is one of the

structural optimization methods developed in applied mathematics (Mutlu and Kayacan 2019).

Topology optimization is the process of changing the distribution of the material within a given design space to create new boundaries, taking into account the loads and constraints on the design to improve the design. Compared to size and shape optimization, topology optimization is used to find an optimal distribution of material without any a priori assumption about geometry with more design freedom (Verbart 2015). The most important reason why designers prefer topology optimization is that the optimum structure can be revealed at the design stage (Albak 2019). A two-dimensional topology optimization used to improve structural performance is seen in Figure 3.4.

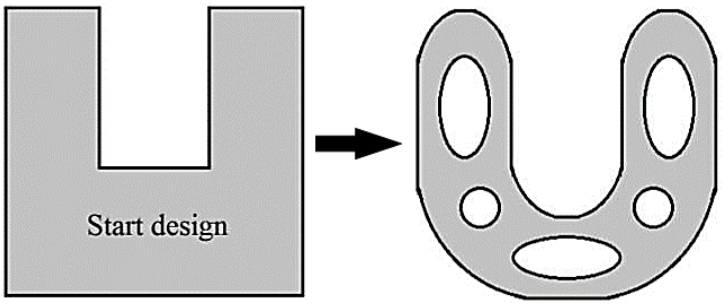

Figure 3.4. Topology optimization
(Source: Abdi 2015)

Topology optimization was introduced firstly by Bendsøe and Kikuchi in 1988 with a homogenization-based method. Within this method, the microstructure is assumed to consist of an infinite number of porous (solids and voids) unit cells that are small and periodically repeating on the microscopic scale (Figure 3.5). The porosity within each element is treated as constant in the FEM and the porosity values are used as design variables in the optimization problem. The main idea of the homogenization-based topology optimization method is to change the porosity depending on where the material is to be removed or kept (Yalamanchili 2012).

The disadvantage of the homogenization-based method is that more design variables are required per element and this situation causes extra processing for the modulus of elasticity of all elements. Furthermore, it makes the problem quite complicated by making the solution hard (Keten 2020). In addition, this method may not

yield the desired continua in that the final continuum may contain many infinitesimal pores making manufacturing hard (Kumar 2017).

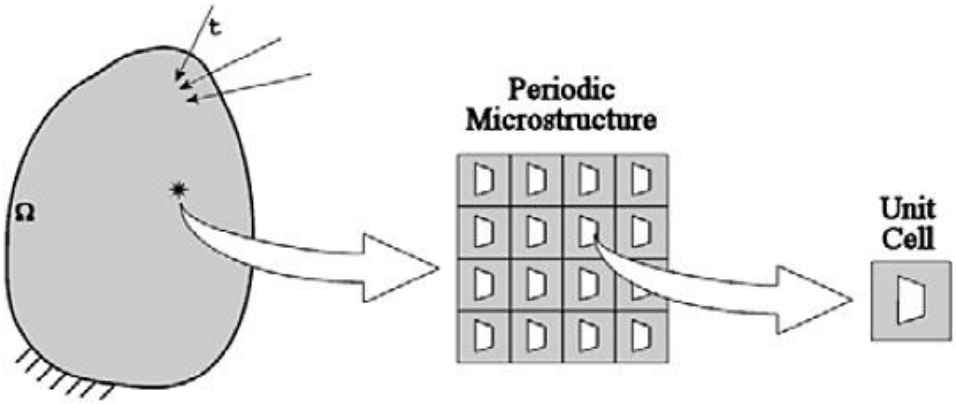

Figure 3.5. Representation of a composite material made of periodic microstructure (Source: Sant'Anna and Fonseca 2002)

For an alternative to homogenization based method, SIMP (Solid Isotropic Material with Penalization) algorithm that is also named density-based method for isotropic materials was proposed by Bondose (1989), Zhou, and Rozvany (1991) and Mlejnek (1992) due to its conceptual simplicity and numerical easiness (Kumar 2016). The main idea of the SIMP method is to convert the discrete feasible domain into a continuum setting which facilitates the use of gradient-based optimization algorithms which are very efficient and computationally less expensive (Yalamanchili, 2012). Furthermore, differ from the homogenization-based method, this approach involves only new material data and it makes the implementation of this approach favorable (Mlejnek 1993; Keten 2020). In addition, fabrication technology can only be implemented in the condition of the variable density method (Li and Wang 2012).

In the density-based method, Lagrangian type rectangular cells are employed to discretize the design space into a large number of finite elements as design variables (Kumar, 2016). Each finite element, x_e is assigned with a relative density vector ρ (Pseudo-density), taking value between 0 to 1. Here, $\rho(x_e) = 0$ is defined voids element that represents material to be removed, $\rho(x_e) = 1$ defined solid element represent the

material to be kept in the structure (Liu, et al. 2018). The representation of this procedure is as shown in Figure 3.6.

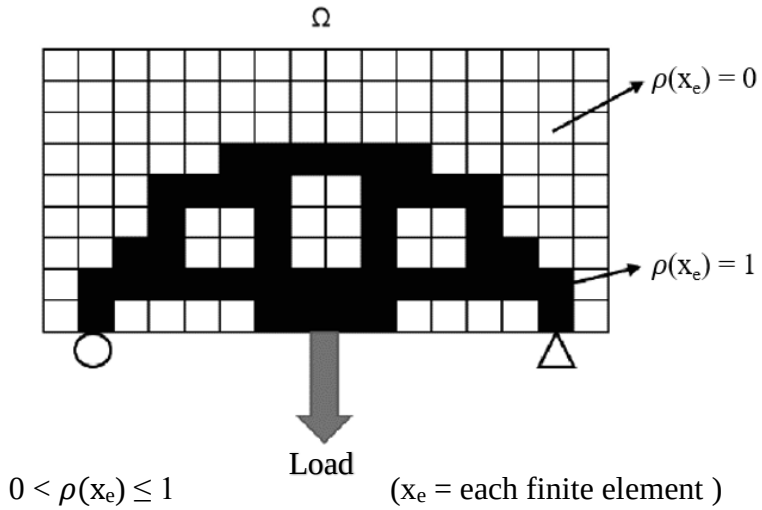

Figure 3.6. Illustration of the density-based topology optimization
(Source: Liu, et al. 2018)

The SIMP algorithm enforces the stiffness of the intermediate densities taking values of relative density ratio closer to either 0 or 1 to obtain better topology patterns with clear boundaries. In addition, this factor suppresses the occurrence of intermediate densities presented in different shades of grey in the optimal design. Geometric representation of a structure as similar to a black-white rendering of an image is shown in Figure 3.7.

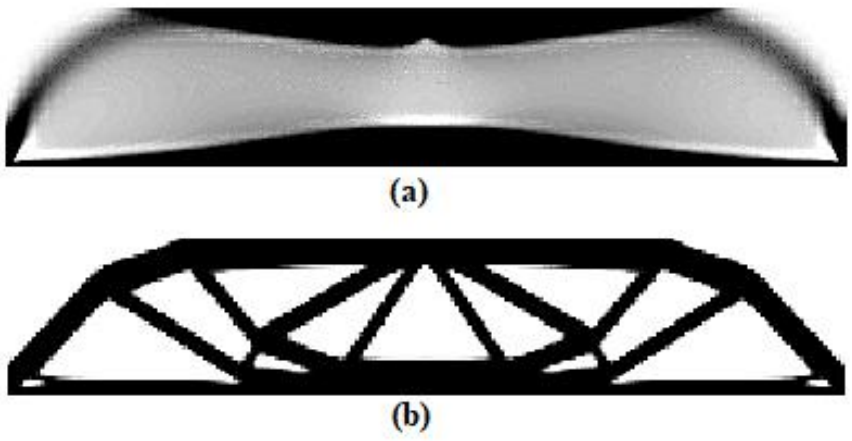

Figure 3.7. Comparison of optimized result with a penalization factor
(Source: Grinde 2018)

It can be seen from Figure 3.7.a, the gray area is a density gradient while the black and white are solid and void, respectively. This gradient is caused by a penalization factor of one being applied so that the density is not forced to change to become a solid or void. In Figure 3.7.b, the density gradient has been penalized for forming black and white, solid and void regions. The solid and void regions can exist because the penalization factor force the density gradients to become solid or void (Grinde 2018; Thummar 2014).

When the penalization parameter is chosen p > 1, the intermediate densities transform into solid and void regions in the final continua because of the decrease in stiffness/volume (relative stiffness) ratio meaning provides little stiffness per volume. So a greater penalty results in a better result. However, the computational time is also increasing while a penalization factor equal to one will result in a density gradient. Without a penalization factor, the resulting beam will have a density gradient while a penalization factor will create a solid and void region. The relation between the relative stiffness and the density according to the different penalization factors is shown in Figure 3.8 (Olason and Tidman 2010).

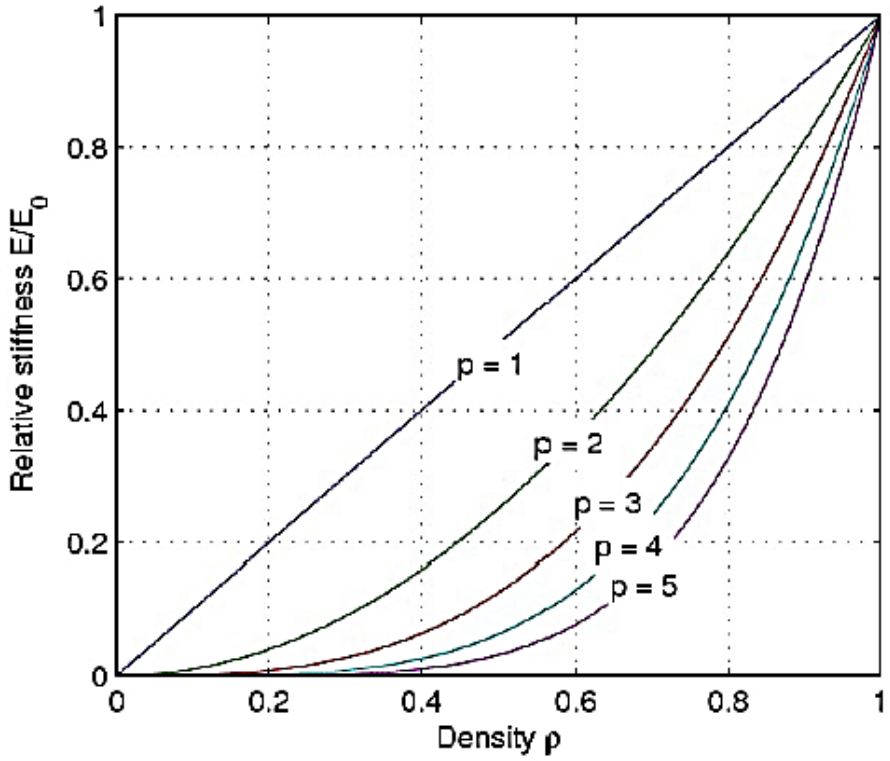

Figure 3.8. Relative stiffness as a function of density with different penalization factors (Source: Olason and Tidman 2010)

The microstructures of intermediate densities constructing from voids and material with the penalization factor limit, p = 3 is shown in Figure 3.9.

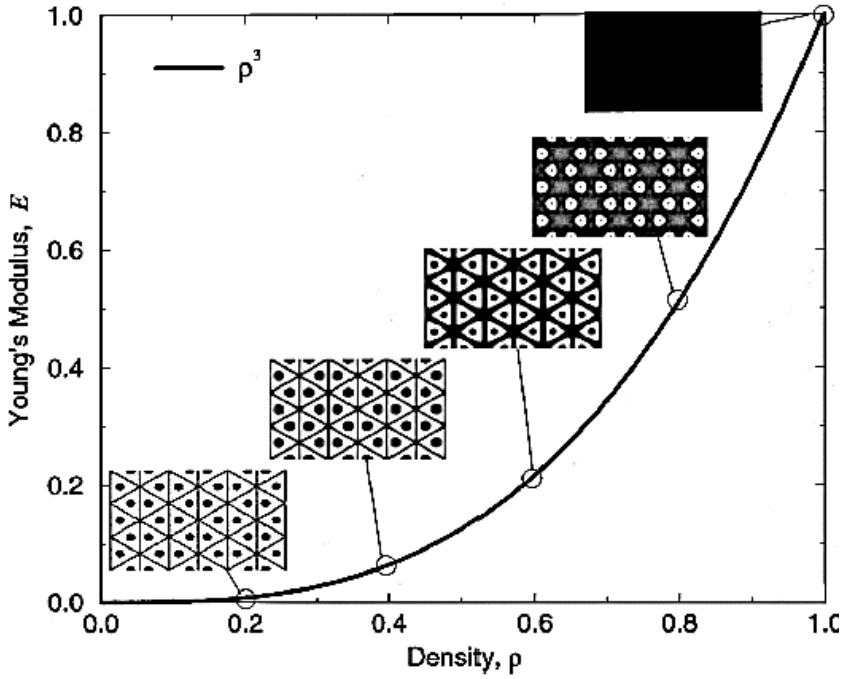

Figure 3.9. Microstructures realizing the material properties with p = 3
(Source: Olason and Tidman 2010)

The material properties are assumed to be related to the relative density of the material. The power-law relation between the relative density ρ_e associated with the element x_e and material properties, E can be expressed as follows:

$$E(\rho(x_e)) = (\rho(x_e))^p E_0 \quad (3.4)$$

where $E(\rho(x_e))$ is an optimized and E_0 is the real Young modulus of a solid material. p is the penalization parameter. Here, E = 0 means that no material exists while E = 1, material exists. Te relative density controls the extent of existing material steered towards 0-1 values by choosing p > 1 (Liu, et al. 2018).

The objective function of any optimization problem can be minimization or maximization of a certain response while meeting a prescribed set of constraints. The

weight is often used as an objective function for single material structures. The weight, W is equivalent to the density scaled volume and calculated by integrating the element densities $\rho(x_e)$ over the design domain, Ω (Thummar 2014).

$$W = \int_{\Omega} \rho(x_e)\, d\Omega \tag{3.5}$$

Based on the SIMP approach, the topology optimization problem under mass minimization considering the stress constraint can be wr as:

Find:

$$\rho(x_e) = (\rho_1, \rho_2, ..., \rho_n) \in R^n \quad , \quad (x_e = 1, 2, \dots n) \tag{3.6}$$

Minimize:

$$W(\rho(x_e)) = \int_{e=1}^{n} \Omega\, \rho(x_e)\, d\Omega \tag{3.7}$$

Subjected to:

$$\sigma\,(\rho(x_e)) \leq \sigma_{max} \tag{3.8}$$

$$0 < \rho_{min} \leq \rho(x_e) \leq 1 \tag{3.9}$$

where *n* represents the total numbers of finite element, m_e is the solid element mass for the element related to design variable x_e, ρ_{min} is the lowest density value limit that cannot

be zero due to causing singularities in the FEA solution, $\sigma(\rho(x_e))$ is allowable stress in the optimization process and σ_{max} is the yield strength of material.

Figure 3.10 demonstrates the work scheme of the SIMP algorithm how is implemented on the computer software. While performing the topology optimization, firstly, the SIMP algorithm uses a uniform distribution of densities (e.g = 0.5) for all elements in the mesh and then, the solver starts the optimization loop by using FEA. In order to evaluate the impact on the objective function with respect to the design variables in terms of a better solution, sensitivity analysis is used. Here, a low-pass filtering technique is applied to update the densities. The updated design variables and the resulting topology is analyzed and optimization is repeated iteratively until desired convergence is reached (Jensen 2018)

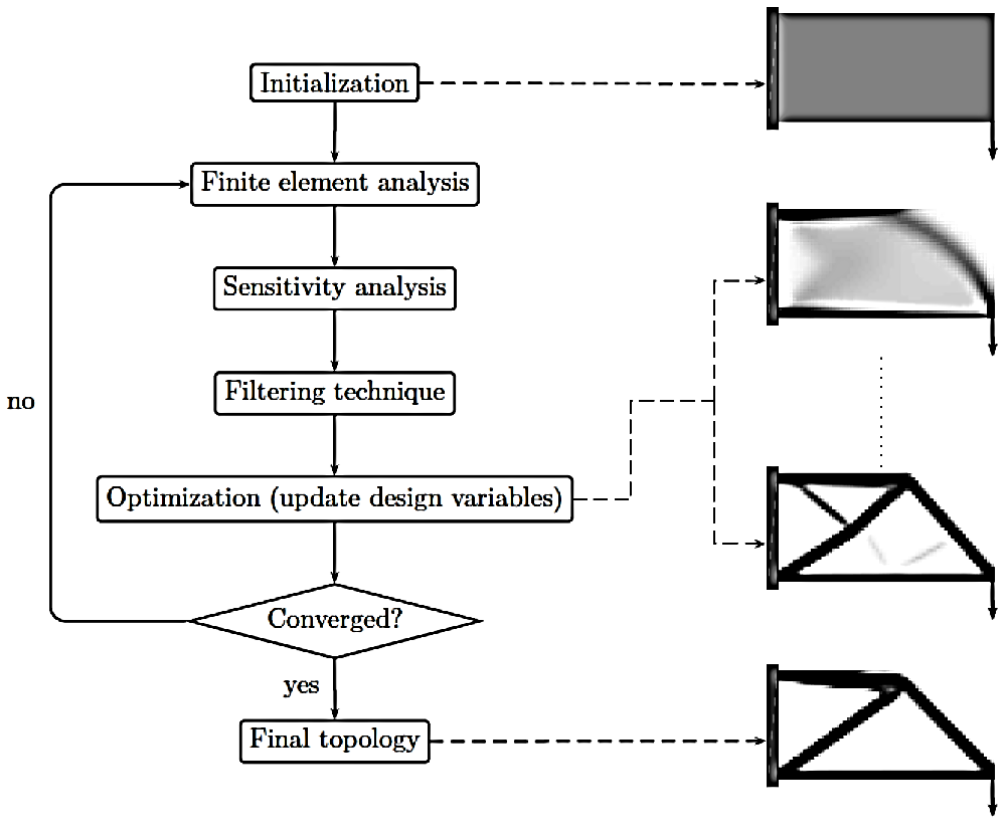

Figure 3.10. Work scheme of topology optimization using the SIMP algorithm (Source: Jensen 2018)

CHAPTER 4

MATERIAL AND METHOD

Structural optimization is a step in the structural design process that aims to increase the structural performance of components and mechanical systems systematically (Sant'Anna and Fonseca 2002). Structural optimization has recently received a wide range of attention in computer-aided engineering (CAE) designs. One of the reasons for rapid development is to help to solve the engineering problems modeled with many complex mathematical equations including reliable analysis capability.

The most widely used solver method in CAE designs is the finite element method (FEM). The FEM is a numerical process that divides structures with complex geometry into very small elements, which cannot be solved manually or by other classical methods. However, in the solutions realized with the FEM, many iterations with a trial-and-error approach are required to reach the final design. Although this effectively meets the design requirements, it may not represent the best solution for the final solution. With the developing computer technology, many analytical solution methods were developed to achieve more efficient results in a shorter time, compared to the trial-and-error approach. Structural optimization methods, which have become widely used in engineering studies in recent years, are one of the methods that provide the best solution in line with this process. The main purpose of these methods is to find a manufacturable design with the minimum material and lowest cost providing the best performance. Among the structural optimization methods, topology optimization is one of the useful techniques that offer ideas to designers without the need for a pre-thought design. In contrast, shape optimization enables the structure obtained as a result of topology optimization to be produced. As a result of the structural optimization methods, structural design can be achieved faster and less costly without requiring physical production in the virtual environment (Sudin, et al. 2014)

The structural optimization adapted CAE designs involves several steps. Hereby, firstly, an initial design space where topology optimization will be performed on an existing or a newly designed structure is created. Considering the working and boundary

conditions of the structure, a FE model of the design space is built. And then, desired and undesired areas where topology optimization to be performed are determined. Furthermore, optimization parameters such as an objective function and design constraints of the structure are defined depending on an optimization problem. The most crucial issue is the definition of the optimization problem affecting optimization results directly. After these definitions, topology optimization is performed and material distribution is obtained depending on the optimization objective and design constraints. Depending on the material distribution obtained from topology optimization, shape optimization is applied to transform this material distribution into a manufacturable form with smooth surfaces. Finally, the new design is achieved with the help of the optimization method and verified with the final FEA. If the obtained results are acceptable, the obtained design is frozen and physical verification tests are performed. Otherwise, the state of convergence to the target is examined and the design process is repeated iteratively until the desired results are obtained (Tyflopoulos, et al. 2018; Munoz 2017).

The optimization steps of the method to be used in this thesis study for structural design is shown in Figure 4.1:

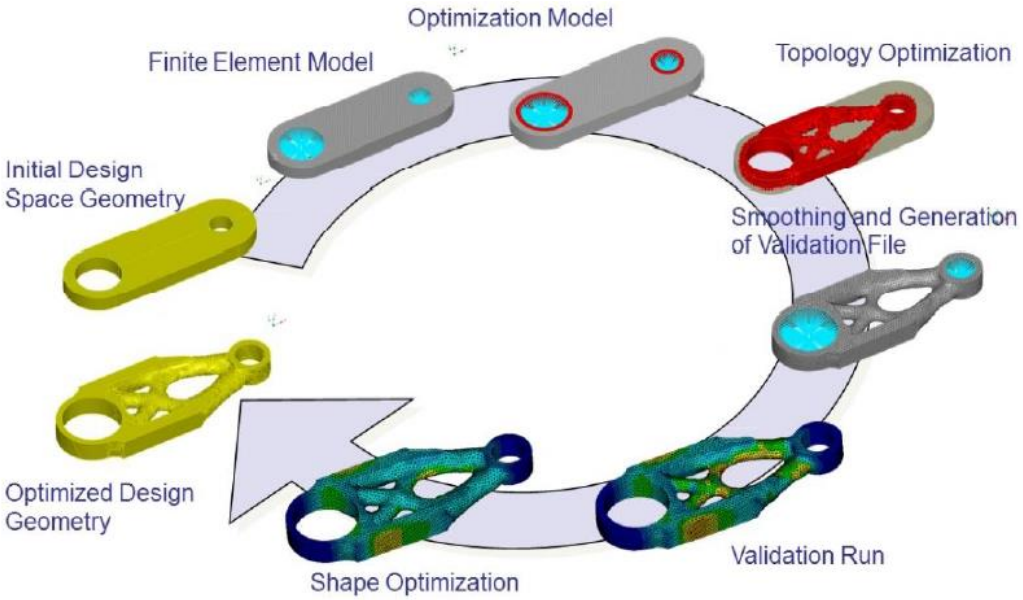

Figure 4.1. Optimization steps for structural design
(Source: Munoz 2017)

In the thesis study, it is intended to design the lightest and high-performance structure instead of the existing shaft bracket with the help of optimization methods that meet the design requirements. Compared with the existing shaft bracket produced with the welding method from metal components, the new structure is proposed to be a monoblock and casting. This casting structure, composed of GGG50 material, must perform reasonable mechanical strength as least as structural steel. Hereby, the new design provides a cost advantage by requiring less engineering time and less production cost. With this purpose, firstly, the three-dimensional design space was created with CAD software, SolidWorks® 2018, according to the vehicle axle application, and then the reaction forces acting on the shaft bracket were calculated for FEA with a kinematic analysis of Z-cam brake. Furthermore, FE model was built depending on the specified boundary conditions and the topology optimization was performed under determined objective function and design constraints with the topology optimization module in ANSYS® 2019 R3 software. With the application of topology optimization, the initial concept design of the desired structure was obtained, and then shape optimization was conducted to bring the distribution into a manufacturable form. For shape optimization, RSM was utilized to obtain the optimal design in ANSYS®. Finally, the FEA of the final design achieved from the optimization process was repeated under the previously determined boundary conditions.

In the following part, the steps of the optimization process for this thesis study have been discussed in detail.

4.1. Define the Initial Design Space and Finite Element Model

4.1.1. Initial Design Space

Before starting the topology optimization process, first, it is necessary to determine the maximum amount of volume known as the design space, according to the vehicle axle platform. This design space represents the volume that will be meshed into finite elements and iterated upon while the optimization process is working (Fornace 2006). In the optimization process, regions, where loads and design constraints are applied, directly affect design and manufacturability of structure. Hence, it is necessary to differentiate the regions. These regions are design region and exclusion (non-design) regions. The

exclusion (non-design) region where loads and boundary constraints are applied is stated as the exclusion(non-design) region where material discharge is not desired meaning these regions can not be removed or modified, while design regions are stated to be removed during the optimization process (Qadeer 2018). Figure 4.2 illustrates the detailed view of the vehicle axle application including the required design space for the shaft bracket to be designed.

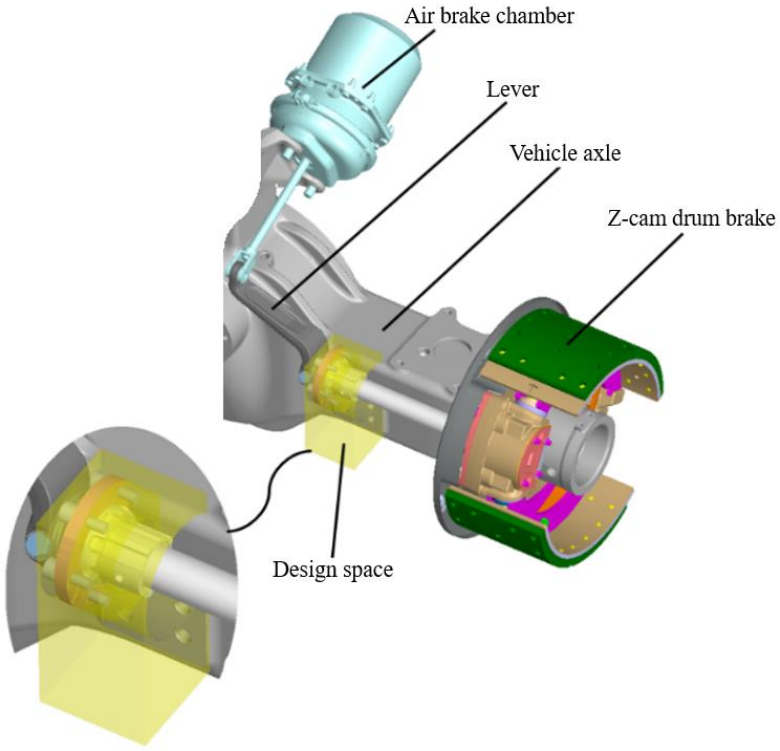

Figure 4.2. The three-dimensional solid model of vehicle axle application
(Source: Ege Fren 2021)

The design space having a volume of 100x100x200 mm^3 was modeled with the 3D software, SolidWorks® 2018, in accordance with the vehicle axle application, shown in Figure 4.3. This design space consists of two different regions, the exclusion (non-design) region and the design region. For the exclusion region, red-colored surfaces represent the bolt holes and mounting surface to ensure the assembly of the shaft bracket to the vehicle axle and the green-colored surfaces represent the bushing mounting region used to

minimize damage on the shaft by reducing the friction during the operation. Other regions are defined as design regions where material discharge can be performed.

In the design space, for geometric discontinuity to be obtained design, the design of fixing hole surfaces must be at least larger twice than the nominal diameter. For that reason, the outer diameters of the bolt holes in the exclusion regions are determined as 30 mm diameter and for bushing hole 110 mm diameter. Furthermore, the distance between the center of bolt holes is set to be 35 mm vertically and 55 mm horizontally. In addition, the mounting surface is determined as an exclusion region, 80 x 100 mm^2. Additionally, to get a more reliable solution in terms of manufacturability, a symmetry plane is added to the middle of the design space. Determining the symmetry plane provides the advantage of the shorter computational time by ensuring that the load applied to the part is distributed equally.

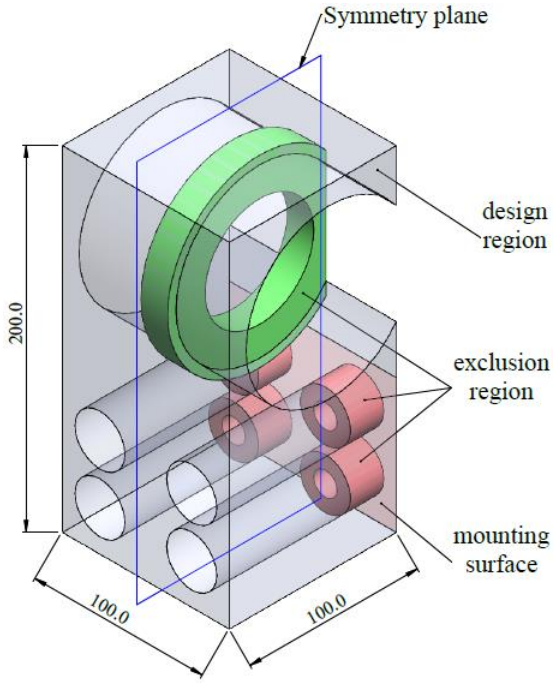

Figure 4.3. Created design space for shaft bracket
(Source: Ege Fren 2021)

After determining the design space, the 3D model created via SolidWorks® is saved in STEP (Standard for the Exchange of Product Data) format, and then imported into the FEA software, ANSYS® 2019 R3 environment to perform the FEA study.

4.1.2. Determination of Boundary Conditions

The shaft bracket is one of the important structural components of the brake system. The shaft bracket not only transfers the chamber force from the brake chamber to the brake shoes but also supports the bearing of the camshaft during its operation. In case of braking, thanks to the braking force generated by the air chamber, the lever mounted on the gear area of the Z-camshaft moves in a circular direction, allowing the shoes to contact the drum. Since the shaft bracket is subjected to high and repetitive loads under braking, it must be as rigid as possible and fulfill its design objectives without any problems and loss of performance during the specified working life. Furthermore, it is extremely important for the performance of the shaft bracket that it has a feature that can absorb vibration loads and will not be damaged depending on working conditions.

After creating design space, it is necessary to determine the loads affecting the shaft bracket by considering the working conditions for FEA. In this sense, the reaction forces acting on the shaft bracket are calculated with the basic schematic diagram of the Z-cam drum brake used in kinematic analysis shown in Figure 4.4. Hereby, to calculate all forces, brake torque (T_b) for the Z-cam drum brake is taken 20 kNm as a reference.

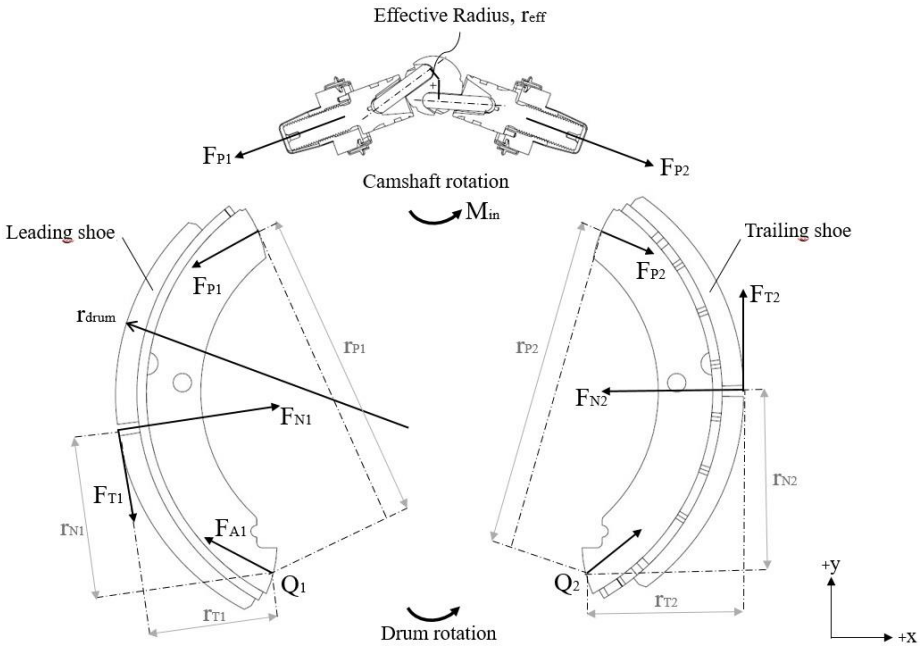

Figure 4.4. Free body diagram of Z-cam brake
(Source: Ege Fren 2021)

In the case of braking, it is assumed that this brake torque is shared equally between the lining and traling shoes of the Z-cam brake. Forces carried out in case of braking due to friction depending on drum direction are stated as F_{T1}, F_{T2} in tangentinal direction center of the lining, F_{N1}, $F_{N2,}$ in normal direciton of the linings; forces F_{A1}, F_{A2} in forces abutment-ends, and F_{P1}, F_{P2} in pistons. The friction coefficient is assumed as μ = 0.37 between the Z-cam drum brake and linings in the calculation (Güleryüz and Yılmaz 2019).

According to Newton second law for force balance equation in counterclockwise direction can be written for leading and trailing shoes as:

$$F_{N1X} - F_{P1X} - F_{A1X} = 0 \quad (4.1)$$

$$F_{A1Y} - F_{T1Y} - F_{P1Y} = 0 \quad (4.2)$$

$$F_{P2X} - F_{A2X} - F_{N2X} = 0 \quad (4.3)$$

$$F_{A2Y} - F_{T2Y} - F_{P2Y} = 0 \quad (4.4)$$

Here, applying moments about Q_1 and Q_2 for leading and trailing shoes, one can reexpress equations (Eq. 4.1 - 4.4) in the following form:

$$F_{N1} \times r_{N1} - F_{T1} \times r_{T1} - F_{P1} \times r_{P1} = 0 \quad (4.5)$$

$$F_{P2} \times r_{P2} - F_{T2} \times r_{T2} - F_{N2} \times r_{N2} = 0 \quad (4.6)$$

where

$$F_{T1\text{-}2} = T_b / (r_{drum}) \quad (4.7)$$

$$F_{N1\text{-}2} = F_{T1\text{-}2} / \mu \quad (4.8)$$

Therefore, the reaction forces acting on Z-cam brake are determined and shown in Table 4.1:

Table 4.1. Calculated reaction forces of Z-cam brake
(Source: Güleryüz and Yılmaz 2019)

Shaft bearing force-leading side, F_{P1}	48864 N
Shaft bearing force-trailing side, F_{P2}	87344 N
Abutment-end force-leading, F_{A1}	117910 N
Abutment-end force-trailing, F_{A2}	35175 N

For the reference brake torque, the required braking force ($F_{chamber}$) must be generated by the air brake chamber under a certain pressure depending on the type (diameter) of the brake chamber. The torque value on the camshaft (M_{in}) is determined by multiplying by effective cam radius ($r_{eff.}$) on the camshaft with the sum of the piston forces (F_{P1}, F_{P2}). Then, the required braking force is obtained as in terms of torque value, lever length (r_{lever}), and air brake chamber efficiency (η) as

$$M_{in} = (F_{P1} + F_{P2}) \text{ x } r_{eff.} \quad (4.9)$$

$$F_{chamber} = M_{in} / (r_{lever} \text{ x } / \eta) \quad (4.10)$$

where the Z-cam system parameters are tabulated in Table 4.2.

Table 4.2. Z-cam brake system parameters

Air chamber force, $F_{chamber}$	15000 N
Shaft moment, M_{in}	1.78 kNm
Lever length, r_{lever}	0.125 m
Effective cam radius, $r_{eff.}$	0.013 m
Air brake chamber efficiency, η	95%

4.1.3. Finite Element Model

The finite element method (FEM) is a numerical approach for solving problems that are mathematically represented by partial differential equations formulated as minimizing a functional (Abdi 2015). This method is widely used in structural mechanics, as it originated as a method of stress analysis in solid structures.

The process begins with the creation of a geometric model. Then, the analysis type should be determined according to the loads to be subjected to the model, time, material type of the model, and desired results. The geometry model subdivides into connected small pieces called meshes. Here, the mesh type must be selected according to the dimensions of the geometry and the type of analysis. Then, the boundary conditions of the finite element model whose element type is determined must be defined. For this purpose, the boundary conditions to be applied to the finite element model should be simulated appropriately regarding the load and boundary conditions in working conditions. Because the accuracy of the results to be obtained directly depends on these conditions (Doğan 2015).

After determining the boundary conditions, the first step is to import the CAD model of the shaft bracket illustrated in Figure 4.3 into the working environment of the ANSYS® Workbench 2019 R3. In the ANSYS® environment, a static structural study is run by dragging from the Analysis Systems column and linked with the imported geometry to the geometry tab of the static structural study and opened the model tab. This linkage in ANSYS® environment is shown in Figure 4.5.

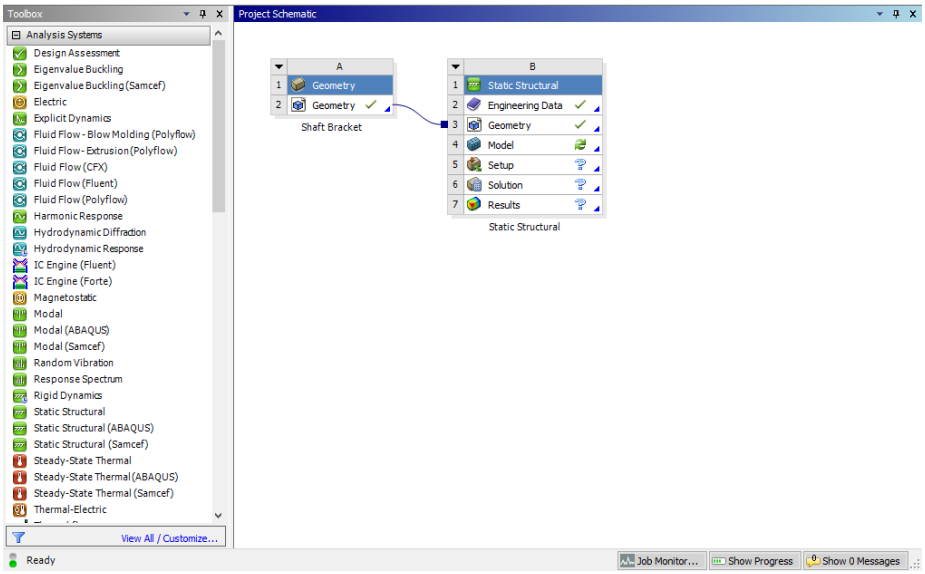

Figure 4.5. ANSYS® Workbench environment
(Source: ANSYS Inc.)

Before initiating the FEA, defining the material properties used in FEA software is a an essential process in terms of the accuracy of the results. After importing the CAD in the software, the material of the shaft bracket is defined from the Engineering Data tab. Because the required material is not directly available in the ANSYS® engineering data source, GGG50 (EN-GJS-500) spheroidal cast iron material is assigned. The material properties of the GGG50 with stress-strain curve is shown in Figure 4.6.

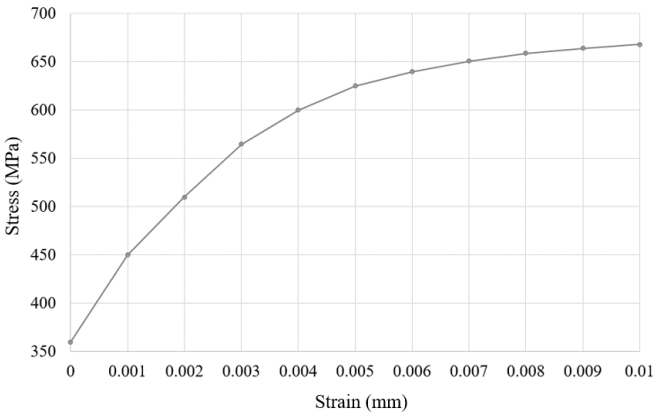

Density	7,3 kg/m3
Young Modulus	170 MPa
Possion Ratio	0.29
Yield Strength	360 MPa
Tensile Strength	500 MPa

Figure 4.6. Material properties of GGG50 with stress–strain curve
(Source: Güleryüz and Yılmaz 2019)

After material identification, the CAD geometry needs to be discretized into several solid elements called mesh for performing the FEA. The meshes are connected to each other at their vertices, which are called a node. The meshing process of the model that will be analyzed using the FEM is a good way to give realistic results. Therefore, meshing quality affects the correct convergence of the result in the analysis process depending on the selected mesh type, mesh size, and the number of the mesh elements and the geometry. The smaller mesh size causes the model to be divided into smaller pieces, increasing both the number of elements used and the accuracy of the analysis results. However, this situation needs a longer computational time. Therefore, despite the lack of an ideal mesh method, the most appropriate method should be chosen for the study by balancing the quality of the mesh with computational time (İpek 2011).

While performing the FEA, different types of meshes are used. Tetrahedral elements are shown in Figure 4.7 which is one of the mesh types that provide many advantages. An arbitrary volume for complicated geometry can always be filled quickly and it can also be easily combined with curvature and proximity size functions to refine the mesh in critical regions.

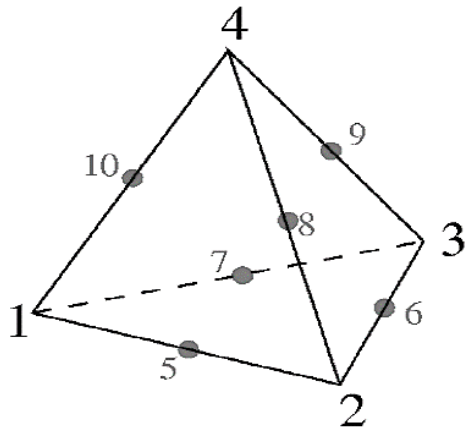

Figure 4.7. Tetrahedral mesh element with 10 nodes
(Source: Özçelik 2011)

Tetrahedron elements that have 4 surfaces and 3 degrees of freedom are composed of triangles. Under normal conditions, solutions can be made with tetra4 elements containing 4 nodes, but these elements cause errors in elongation and stress results.

Instead, tetra10 elements are created by adding nodes to quadratic points. As a result, tetra10 elements have greater degrees of freedom (Özçelik 2011).

A mesh discretization and refinement strategy have been generated in the ANSYS® Workbench environment. The finite element mesh is constructed out of second-order tetrahedral elements using a target element size of 3 mm, applied to all shaft bracket surfaces with performing mesh refinement as shown in Fig. 4.8. The model consists of 317193 nodes and 204494 elements.

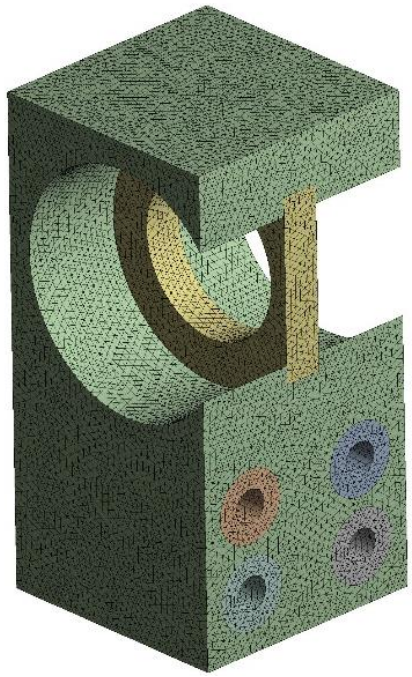

Figure 4.8. FE model of design space with tetrahedral mesh elements

Average element quality and skewness are among the factors to be taken into account in FEA. These values should be checked in terms of the accuracy of the result to be obtained after meshing. The average element quality above 80% is sufficient for the accuracy of the finite element analysis result. Another issue is the skewness value. The skewness value takes a value between 0 and 1, and as this value approaches 0, the quality of the mesh structure increases. If these values cannot be obtained, improvements should be made in the meshing process (Ansys 2013). In this study, the average element quality

is 81% and the skewness is 0.14 according to the used mesh metric. These values are sufficient for accurate results and resolution time.

The existing shaft bracket is mounted to the torque plate by fixation bolts. However, the new design shaft bracket for application is mounted on the vehicle axle directly, as shown in Figure 4.2, instead of the torque plate. Considering this situation, the created suitable design space for the vehicle axle application is fixed by applying for fix support from the bolt hole surfaces. The calculated air chamber force ($F_{chamber}$) in Table 4.2 is applied on the inner surface of the bushing mounting region as a bearing load in a perpendicular direction depending on the assembly position of the air brake chamber on the vehicle axle. The boundary conditions of FEA is shown in Figure 4.9

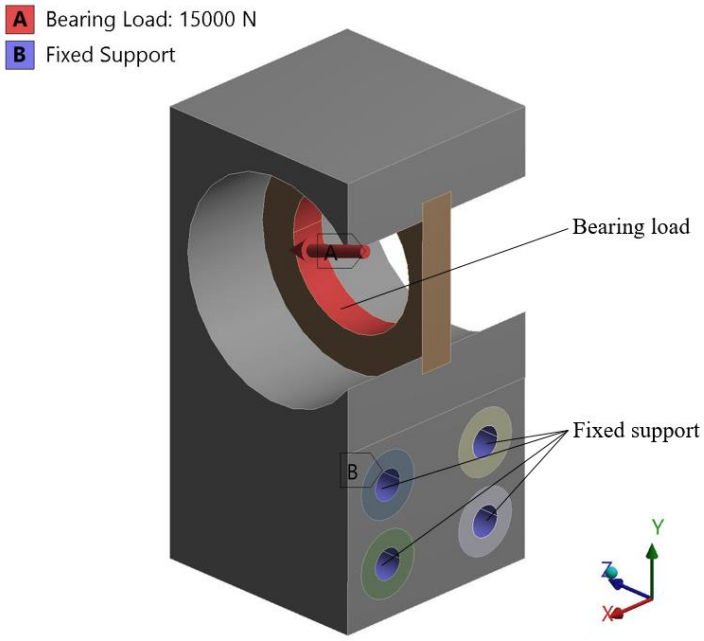

Figure 4.9. Applied boundary condition on design space for FEA

4.2. Topology Optimization Process

An engineering design problem has more than one acceptable design solution and the purpose of topology optimization is to choose the best among the different acceptable solutions. For topology optimization to give an accurate result, the design variable, design constraints, and purpose of optimization must be correctly defined (Yıldız, et al. 2004).

Topology optimization adapted to the CAD is an iterative procedure. The main purpose of this method is to achieve an optimal material distribution that exhibits the best structural performance within the available volume of the structure, depending on boundary conditions and design constraints.

In the thesis study, the topology optimization was conducted using ANSYS® 2019 R3 software that includes a direct topological optimization module that greatly simplifies the steps required to analyze an improved user interface that offers effective user-machine communication. ANSYS® performs material distribution by using the SIMP material distribution method, to allow material discharge where stress is reduced or deleted, while preserving the material structure where stress is high.

To perform the topology optimization, a topology optimization module is dragged from the Analysis Systems column and then linked to the solution of static analysis. As a result, engineering data, geometry and model tabs are directly joined at the same time. The topology optimization setup in ANSYS® environment is shown in Figure 4.10.

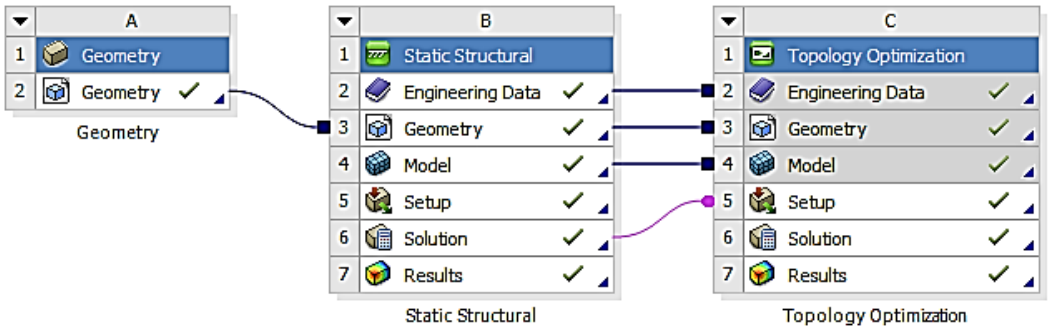

Figure 4.10. Topology optimization setup of the shaft bracket in ANSYS® environment (Source: ANSYS Inc.)

The topology optimization procedure consists of the following main steps:

Step 1: define analysis settings

Step 2: determine optimization regions

Step 3: determine objective

Step 4: determine response constraint

Step 5: determine manufacturing constraints

For step 1, define analysis settings. Defining the optimization parameters according to the design target is vital in terms of the accuracy of the solution. Firstly, a maximum number of iterations is set. By default, the maximum number of iterations is defined as 500 in ANSYS®, but it can be changed to another desired number optionally. This number states the maximum number of iterations that the solver will iterate until it converges.

For numerical reasons, the density of an element can not exactly be zero. Therefore, the minimum normalized density has to be specified and it can be of any value between 0 and 1. By default, it is set to 0.001. The convergence accuracy can be increased or decreased according to the desired precision. The default value is used as 0.1%, however, a higher value can be applied to studies that require improved accuracy. For that reason, the convergence accuracy is recommended as 0.05% for the objective mass minimization.

Sequential Convex Programming (SCP) is chosen as a solver type. Penalty factor has to be specified in order to steer the solution to a 0-1 optimized geometry. The penalty factor is recommended to be set to 3. This prevents the structural stiffness matrix from scaling linearly with the pseudo density (Jensen 2018).

Analysis settings used in ANSYS® for topology optimization are shown in Figure 4.11.

Definiton	
Maximum Number Of Iterations	500,
Minimum Normalized Density	1,e-003
Convergence Accuracy	5,e-002%
Penalty Factor (Stiffness)	3,
Region of Manufacturing Constraint	Include Exclusions
Region of Min Member Size	Exclude Exclusions
Region of AM Overhang Constraint	Exclude Exclusions
Solver Controls	
Solver Type	Sequential Convex Programming
Output Controls	
Store Results At	All Iterations

Figure 4.11. Analysis settings of topology optimization

For step 2, determine optimization regions. In order to perform the topology optimization accurately, determining regions to be optimized or not is important. ANSYS® sets the entire model as a design region by default. However, It is necessary to differentiate the regions to be optimized because the regions on which we will apply load and constraints cannot be optimized and will not be changed by the software.

For determining these optimization regions in ANSYS® environment, firstly, all bodies are selected as geometry located under the design region column. Hereby, the design region are represented with blue-colored. Then, to differantiate the all specified surfaces of exclusion region in Figure 4.3 mening not be optimized are selected under the exclusion region column and represented with red-colored. Finally, the optimization type is selected as density-based. The definition of regions used in ANSYS® environment is shown in Figure 4.12.

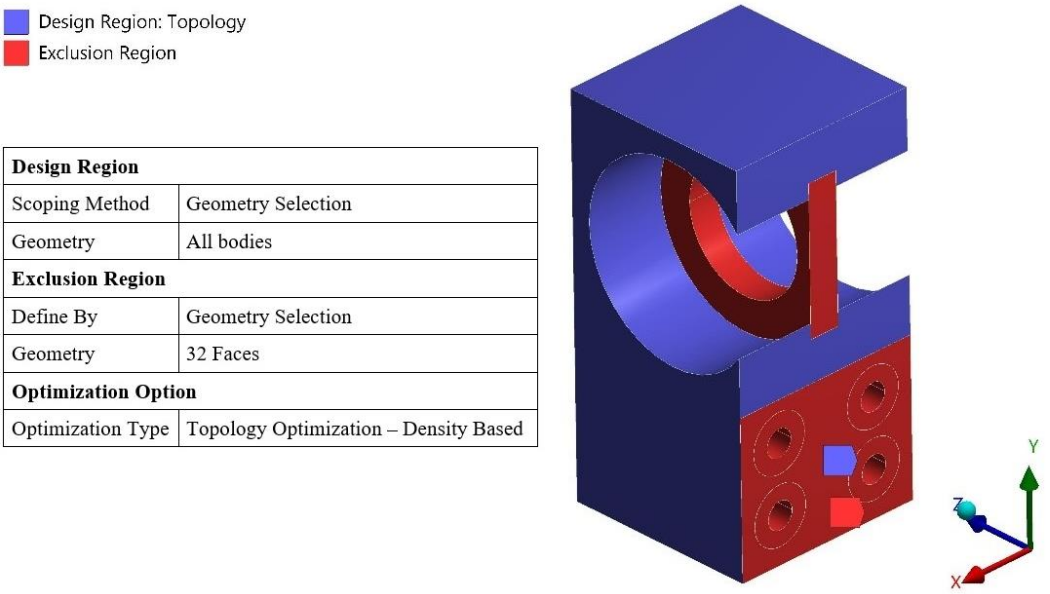

Design Region	
Scoping Method	Geometry Selection
Geometry	All bodies
Exclusion Region	
Define By	Geometry Selection
Geometry	32 Faces
Optimization Option	
Optimization Type	Topology Optimization – Density Based

Figure 4.12. Optimization regions of the shaft bracket geometry

For step 3, determine the objective. The objective function of any optimization problem can be defined as minimization or maximization of a certain response within given design constraints (Sudin, et al. 2014). Here, the structural topology optimization problem is generally stated as compliance minimization with respect to the volume or weight fraction. Although this method provides satisfying results, there are several disadvantages of using compliance as the criteria of design structures. Because the amount of material to be removed with compliance minimization is obtained independently from the stress constraint and this situation does not show the same performance with the lowest maximum stress. Due to the stress is a parameter affecting the structure properties, stress cannot be evaluated in detail in the obtained design using compliance minimization. In addition, in practical application, the compliance minimization requires predefined constraint such as volume fraction (Yalamanchili 2012)

ANSYS® has three different objectives for minimization or maximization of problems such as compliance, mass, or volume. For this study, the objective function is defined as the minimization of the mass. Here, under the objective function, the mass is reduced by removing the material from the part geometry iteratively to achieve the maximum rigidity with the minimum amount of material.

For step 4, determine the response constraint. ANSYS® has a set of constraints that the solver has to take into account when optimizing the geometry. Its response constraint can control the desired response during an optimization. Under response constraint, stress is selected depending on the optimization objective and the allowable equivalent stress limit is defined as 350 MPa with respect to the yield point of GGG50 material. This value is arbitrarily set, and it is limited by the maximum amount of material that can be removed while complying with the boundary conditions set.

The definition of response constraint in the ANSYS® environment used for topology optimization is shown in Figure 4.13.

Scope	
Scoping Method	Optimization Region
Optimization Region Selection	Optimization Region
Definiton	
Type	Response Constraint
Response	Global von-Mises Stress
Maximum	350, MPa
Environment Selection	All Static Structural
Suppressed	No

Figure 4.13. Response constraint of topology optimization

For step 5, determine manufacturing constraints. Pull-out direction and other manufacturability considerations for the casting process are vital. For that reason, in terms of manufacturability considerations, the minimum member size allowed on the geometry is determined as 7 mm and this value is represented as the minimum thickness value desired on the part after optimization. In addition, the symmetry constraint is set and the axis that is desired to take place is defined in the program as the x-axis with respect to the pull out direction in order to make the material unloading operation equally. Applying the symmetry plane reduces by equally distributing the load acting on the bracket. It also gets faster results allowing a more robust structure by giving a greater resistance and stability to the optimized piece (Qadeer 2018). The definition of the manufacturing constraints for the shaft bracket geometry is shown in Figure 4.14.

Scope	
Scoping Method	Optimization Region
Optimization Region Selection	Optimization Region
Definiton	
Type	Manufacturing Constraint
Subtype	Member Size
Suppressed	No
Member Size	
Minimum	Manual
Min size	7,mm
Maximum	Program Controlled

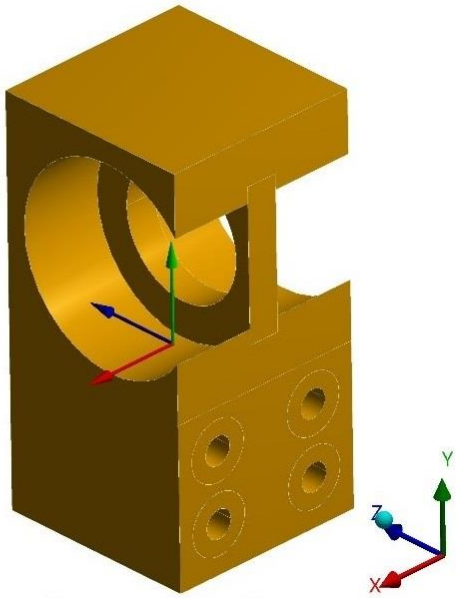

Figure 4.14. Manufacturing constraints of the shaft bracket geometry

All defined parameters used for topology optimization procedure in ANSYS® environment is summarized in Table 4.3.

Table 4.3. Parameters of topology optimization problem

Objective	Mass minimization
Response Constraint	Stress (≤ 350 MPa)
Manufacturing Constraints	Symmetry (x-plane) Minimum member size (≥ 7 mm)

4.3. Material Removal Process

According to the results of topology optimization, the surfaces of the structure are rough and it is needed to have smoothed features in terms of manufacturable form based on material distribution. Here, Space Claim integrated into ANSYS® is a CAD software

is being capable of modeling solutions. The main purpose is to read STL file exported from topology optimization and redefine the geometry before design validation (Jensen, 2018). After topology optimization, the optimization result was exported as an STL file into the Space Claim environment and the initial producible geometry in Figure 4.15 was created by considering the manufacturing constraints such as parting line, draft angle and fillet of radius for the shaft bracket. After the model is redesigned with smoothing features, it is used for shape optimization to meet the design requirements effectively compared to the initial model.

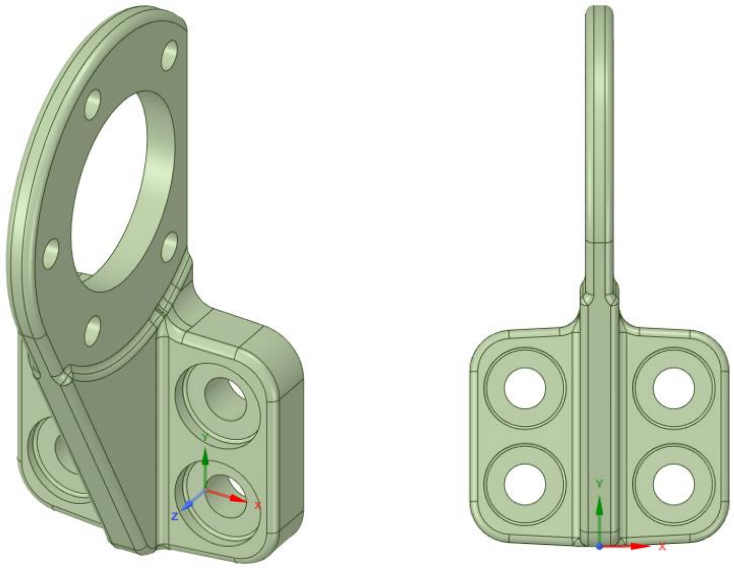

Figure 4.15. Created initial concept design after topology optimization

4.4. Shape Optimization Process

It is not possible directly to use the material distribution generated after the topology optimization and the material distribution result of the structure must be turned into a realistically manufacturable way by keeping constant the topology. The design to be obtained should have the lowest mass versus the lowest amount of strain and stress. In line with this purpose, shape optimization ensures that the dimensions of the structure are optimized under the specified target (Doğan 2015). Hereby, different design parameters such as thickness, width, fillet radius, length of the part are defined parametrically and

examined to use the structural domain more effectively by changing the number and the configuration of the structure until design requirements are met.

There is a relation between design parameters of structure and system responses such as mass, stress, and deformation under defined conditions. In the structural design, in order to provide a condition in which the best result can be obtained examining the effects of design parameters on system responses, experimental studies such as Response Surface Method (RSM), Design of Experiments (DOE) are preferred.

DOE is a systematic method that helps to explore, understand, and optimize changing the range of values of the design parameters in the same set of experiments. DOE is a powerful data collection and analysis tool to get perfect experimental results maximizing the amount of information gained from a limited number of samples while minimizing the amount of data to be chosen in the design space. The objective of DOE is the selection of the design points where the response should be evaluated (Menon, 2005)

RSM is a statistical method including mathematical approximation that was first developed by Box and Wilson in 1951. The RSM is considered shape optimization and used to demonstrate responses having a potential effect on design parameters by creating a response surface function in accordance with the specific rules of sampling parameters (Menon, 2005). RSM associated with DOE is used to define the effect of the input-output based on a set of data samples generated with a mathematical function.

In structural design optimization with RSM, it is necessary to estimate the mathematical form of the function between the response and the design parameters. For that reason, generally, the second-order polynomial regression model is preferred to obtain better results. The unknown coefficients in the model are approximated using the method of least squares (Menon, 2005).

In RSM methodology, the quantitative form of relationship between the response function and two independent design parameters can be defined as follows (Menon, 2005):

$$Y = \beta_0 + \sum_{j=1}^{k} \beta_j x_j + \sum_{j=1}^{k} \beta_{jj} x_j^2 + \sum_{i \neq j}^{k} \beta_{ij} x_i x_j + \varepsilon \qquad (4.11)$$

The response vector, Y is a function of the design parameters that is also called independent design variables x_j, k is number of design varible, ε, the experimental error

and β_0, β_j, β_{ij}, regression coefficients respectively (Menon, 2005).

DesignXplorer™ module integrated into ANSYS® is one of the most advanced optimization tools for conducting experimental studies in computer simulations and is widely used o generate automatic sample points in the optimization process in the engineering industry as well as in a variety of research fields. DesignXplorer™ effectively identifies the relationship between the design variables and the desired performance of a model (Munoz 2017).

The basic shape optimization setup using the DesignXplorer™ module in ANSYS® is shown in Figure 4.16. The desired method to be used for the optimization is selected from the design exploration toolbox by dragging and linking with the parameter set.

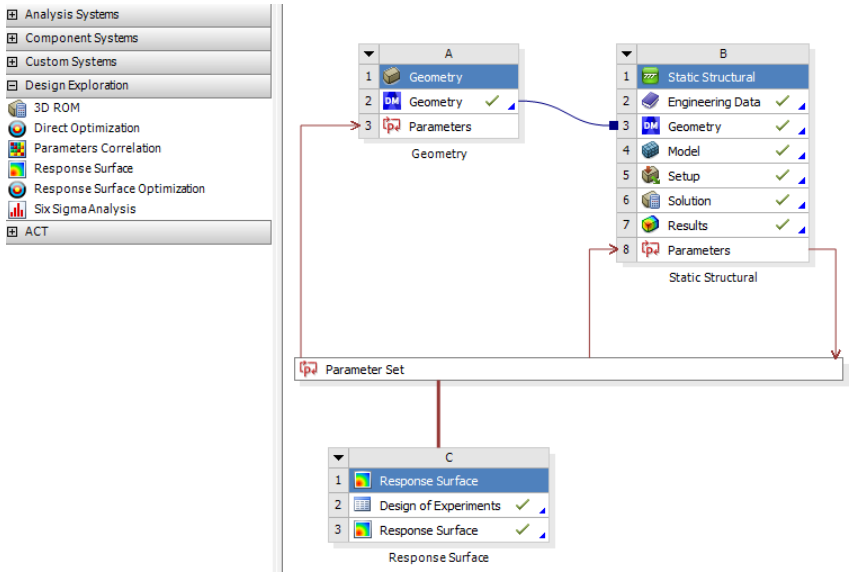

Figure 4.16. Optimization setup with DesignXplorer™ module in ANSYS® (Source: ANSYS Inc.)

The shape optimization procedure consists of following main steps:

Step 1: definition of factors and responses

Step 2: selection of design exploration method

Step 3: selection of DOE method

Step 4: creation of a response surface

Step 5: sensivity analysis of the results

Step 6: design optimization

For step 1, define of factors and responses. In order to conduct shape optimization for a given model, firstly, design parameters which will be optimized called input and responses called output are defined. In an engineering design process, it is very important to know what input parameters, and how many of these, are factors that influence in some way output parameters, and then decide which input parameters should be considered (Salem 2017).

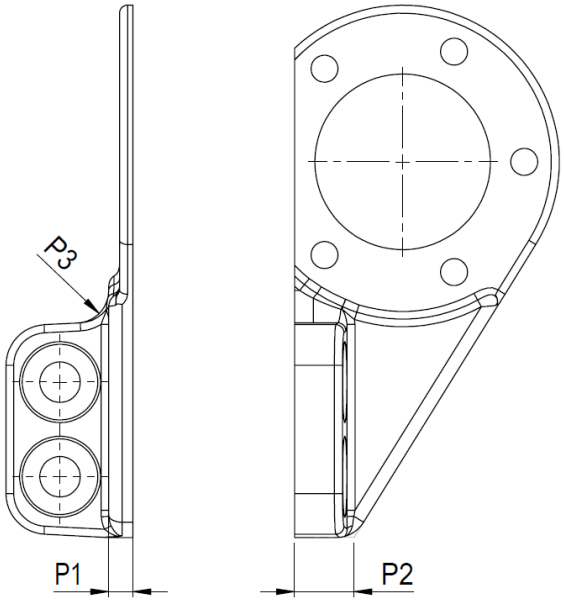

Figure 4.17. Design parameters to be optimized
(Source: Ege Fren 2021)

The created design via Space Claim shown in Figure 4.17 was chosen as an empirical model for the shape optimization process. Here, for the shape optimization process of the shaft bracket, the half model was considered to realize the solution process quickly and make the parametric definitions conveniently in FEA. This was preferred because the shaft bracket had axially symmetric geometry.

For shape optimization of the new design shaft bracket, three different critical design parameters affecting the weight, stress and deformation of structure have been investigated. These are support thickness (P1), support length (P2) and radius of fillet (P3), shown in Figure 4.17. In accordance with the upper and lower limits of these variables, design points were specified by parametrizing. Here, P1 is varied between 7-9

mm, P2, 22-26 mm and P3, 8-12 mm with the help of DOE. Then, weight, equivalent stress and total deformation are investigated as the desired responses.

For step 2, select the design exploration method. In this study, in order to perform shape optimization, RSM is applied. Response Surface tab located in Design Exploration Toolbox is linked with the parametric study defined in step 1 by dragging into the ANSYS® environment as shown Figure 4.18. This will allow to perform DOE to create a predictive model, called a response surface.

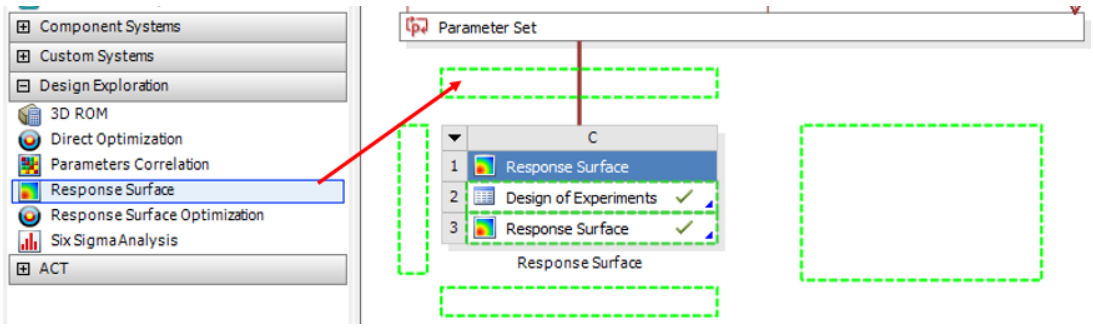

Figure 4.18. Response surface tab in ANSYS® Workbench environment (Source: ANSYS Inc.)

For step 3, select an appropriate DOE method for the problem. ANSYS® proposes various DOE methods to fit response surface such as, Central Composite Design (CCD), Box Behnken Design (BBD), Optimal Space Filling Design (OSFD) (it is also called D-optimal Design), Full Factorial Design (FFD), Latin Hypercube Sampling Design (LHSD) (Ren and Vipradas 2021). In this study, Optimal Space Filling Design (OSFD) was selected. D-optimal experimental design is response surface based methodology, used for conducting the design of experiments, the analysis of variance, and the empirical modelling, and this method has some advantages compared to other response surface methods (Kuram, et al. 2013). This procedure generates D-optimal designs for multi-factor experiments with both quantitative and qualitative factors. A selection method creates the finest design based on a chosen factor and a specified amount of test runs. This approach is especially helpful if classical design methods are not being used (Erten, et al. 2020). The main advantage of these methods is that the number of samples is independent from the number of parameters.

According to the experimental design with the help of ANSYS®, 15 design points were determined by the OSFD (D-optimal) depending on identified input design parameters and shown in Table 4.5.

Table 4.4. Result of Optimal Space Filling Design (OSFD)

	Thickness, P1 (mm)	**Length, P2 (mm)**	**Fillet, P3 (mm)**
1	7.733	25.333	11.067
2	7.200	23.467	11.333
3	8.533	22.400	10.533
4	8.400	25.067	8.400
5	8.133	22.133	8.667
6	7.733	25.867	9.467
7	7.067	24.533	9.200
8	8.667	25.600	10.267
9	7.867	24.267	9.733
10	8.933	24.000	10.800
11	8.000	22.933	11.867
12	7.467	22.667	10.000
13	7.600	23.733	8.133
14	8.267	24.800	11.600
15	8.800	23.200	8.933

For step 4, create the response surface. The DOE results were used to create a response surface for prediction purposes. ANSYS® provides different response surface methods for the regression analysis: Standard Response Surface (It is also called 2nd order polynomial), Kriging, Non-parametric Regression, Neural Network, Sparse Grid. For this study, the Standard Response Surface method was used. It requires the least amount of computation in both fitting and prediction. This method uses a polynomial model to fit the data points by using the least square methodology. The points generated on the response surface are then used to perform the optimization (Ren and Vipradas 2021).

For step 5, the sensitivity analysis is carried out in order to illustrate the relationship between inputs and outputs. This suggests that whether there is a strong correlation between all the selected inputs and the specified outputs. Moreover, major effects on the output parameters can be determined.

For step 6, the created prediction models can be used for shape optimization.

CHAPTER 5

RESULTS AND DISCUSSION

5.1. Optimization

The main idea behind the topology optimization is to distribute the densities of each element in the design space between 0 and 1. These values represent the void and solid material density of each element. This gives an idea to designer about the structure. Low-density value represents a void that must be removed from the structure and high-density value indicates solid material that must be kept in the structure (Fornace 2006). After performing topology optimization, the optimal material distribution satisfying design limits and objectives can be obtained.

The material density distribution of the shaft bracket is shown in Figure 5.1 after 135 design iterations using ANSYS® 2019 R3 the topology optimization module.

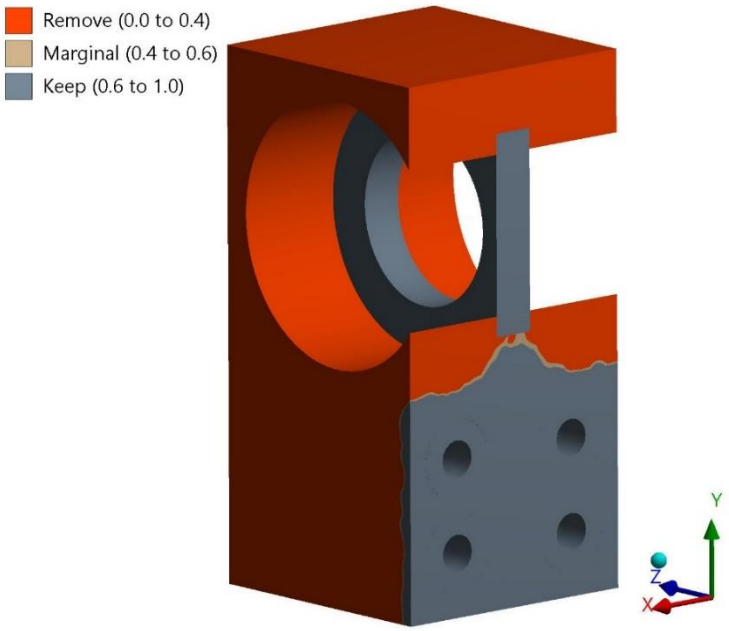

Figure 5.1. Material density distribution of topology optimization for shaft bracket

In order to visualize the density values of topology optimization results in the graphics view, the default retained threshold value is taken as 0.5. Besides, depending on density values of topology optimization ranged from 0 to 1.0, the red-colored region named remove indicates a retained threshold value of 0 to 0.4, the yellow-colored region named marginal indicates a value of 0.4 to 0.6, and the gray-colored region named keep indicates a value greater than 0.6.

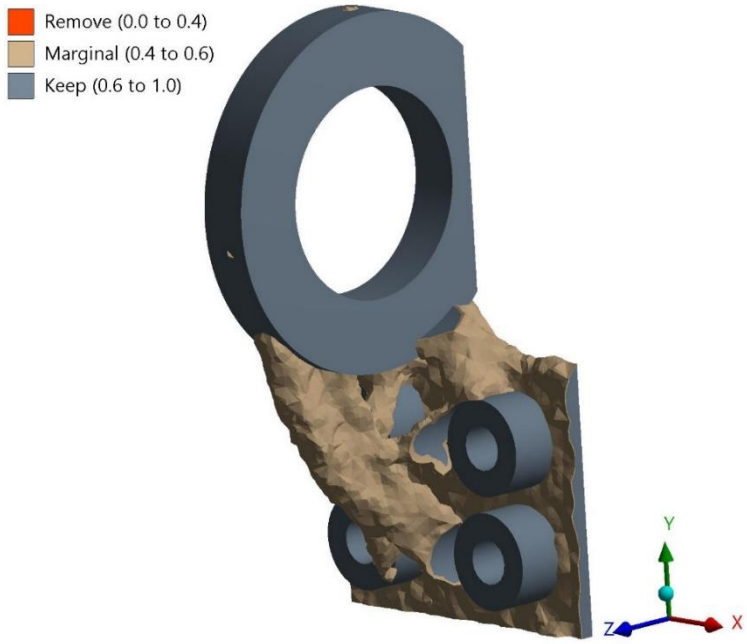

Figure 5.2. Topology optimization result for shaft bracket under 0.5 threshold

According to the topology optimization result, it can be clearly observed from the figures that the materials have only been removed from the assigned design region whereas the exclusion regions as in non-design space remain unchanged.

The created design by Space Claim illustrated in Figure 5.3 was chosen as an empiric model for the shape optimization process. Depending on the new model, three different critical design parameters, support thickness (P1), support length (P2), and

radius of fillet (P3), affecting the weight, stress and deformation, have been investigated as shown in Figure 5.3.

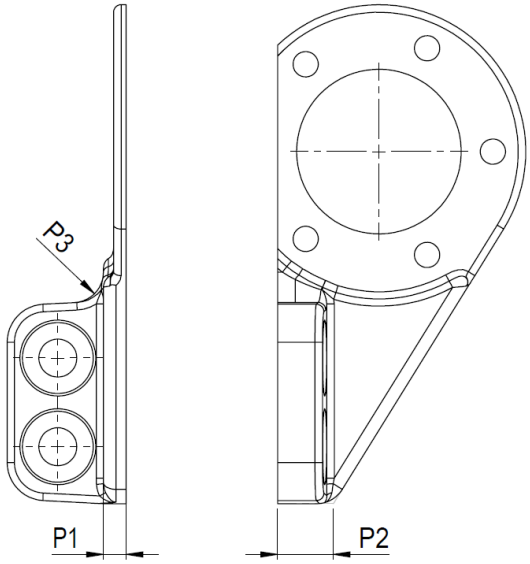

Figure 5.3. Design parameters for the shape optimization process

In accordance with the upper and lower limits of these variables (Table 5.1), the design points were specified.

Table 5.1. Upper and lower limits of design variables

Design Parameters	**Lower Limit (mm)**	**Upper Limit (mm)**
Support thickness, P1	7	9
Support length, P2	22	26
Radius of fillet, P3	8	12

As a result of the DOE-based optimization, the DesignXplorer™ module is suggested the fifteen design points which consist of the combination of numerous values of parameters. The results of all the implemented simulations were summarized in the Table 5.2. The output responses given in Table are investigated with the help of FEA.

Table 5.2. DOE-OSFD results for shape optimization

	Input Desing Variables			**Output Responses**		
Design Points	**Support Thickness, P1 (mm)**	**Support Length, P2 (mm)**	**Radius of Fillet, P3 (mm)**	**Equivalent Stress (MPa)**	**Total Deformation (mm)**	**Total Weight (kg)**
1	7.733	25.333	11.067	266.28	0.67	1.75
2	7.200	23.467	11.333	275.65	0.69	1.72
3	8.533	22.400	10.533	234.70	0.62	1.88
4	8.400	25.067	8.400	232.63	0.61	1.88
5	8.133	22.133	8.667	247.21	0.65	1.83
6	7.733	25.867	9.467	250.89	0.65	1.82
7	7.067	24.533	9.200	277.85	0.70	1.72
8	8.667	25.600	10.267	229.93	0.60	1.92
9	7.867	24.267	9.733	250.70	0.65	1.81
10	8.933	24.000	10.800	225.25	0.59	1.94
11	8.000	22.933	11.867	249.72	0.65	1.82
12	7.467	22.667	10.000	267.19	0.68	1.76
13	7.600	23.733	8.133	260.25	0.67	1.78
14	8.267	24.800	11.600	237.17	0.62	1.86
15	8.800	23.200	8.933	226.52	0.60	1.92

Sensitivity analysis of DOE results is evaluated by plotting Goodness of fit for all the three outputs: weight, equivalent stress, and total deformation (Figure 5.4). It can be seen from the figure that there is no significant deviation in all outputs. This indicates that the DOE results can be acceptable for shape optimization.

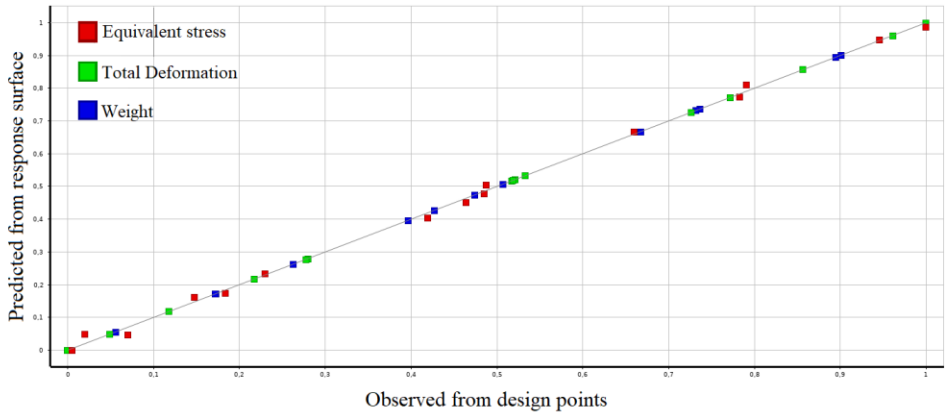

Figure 5.4. Goodness of fit for design points on predicted response surface

Output responses based on second order polynomial are presented in three different graphs as functions of equivalent stress, total deformation and weight of geometry shown in Figures 5.5, 5.6 and 5.7, respectively.

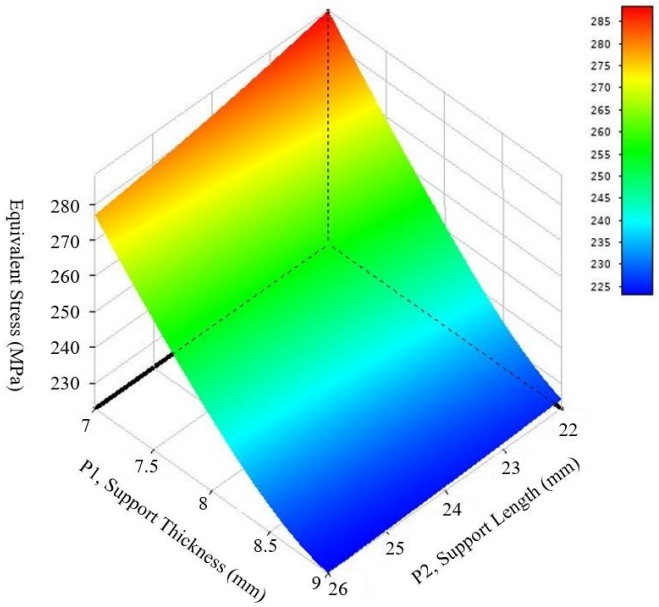

Figure 5.5. Output response surface for equivalent stress

As shown in Figure 5.5, the equivalent stress responses are constructed in defined structural limits given in Table 5.1. According to the result, the equivalent stress value on the geometry decreases considerably when the support thickness increases from 7 mm to 9 mm. However, an increase of support length does not affect the equivalent stress so much as support thickness.

Figure 5.6 shows total deformation responses. According to the result, total deformation value decreases when the support thickness increases from 7 mm to 9 mm. Additionally, an increase in support length has a significant effect on the total deformation, unlike equivalent stress response.

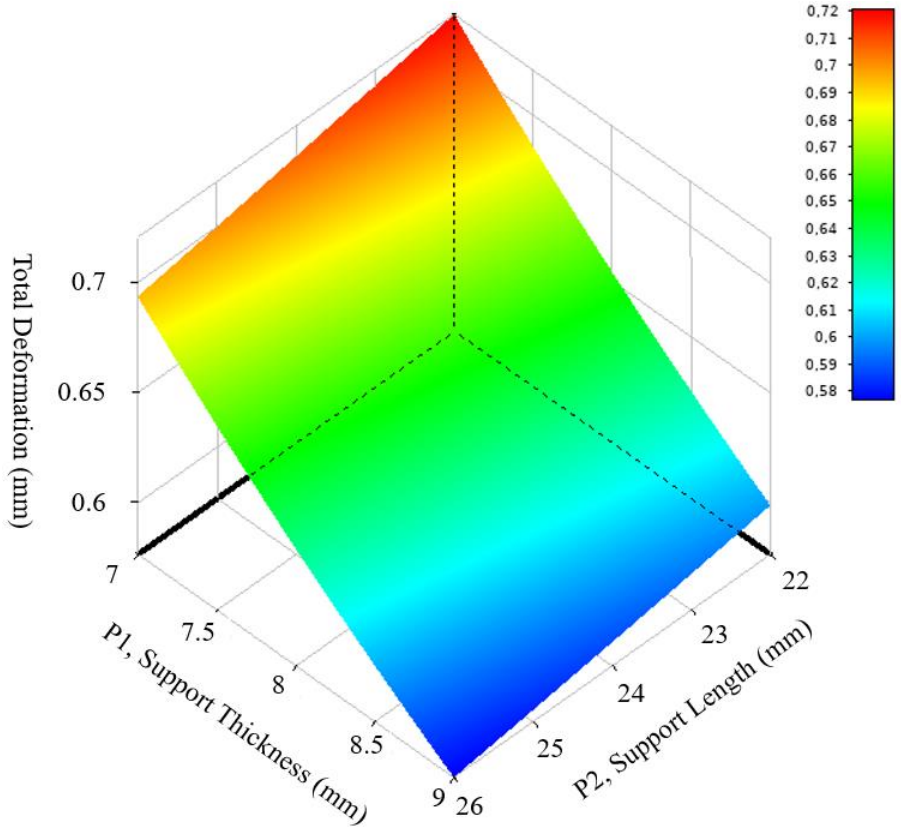

Figure 5.6. Output response surface for total deformation

The weight of geometry responses is shown in Figure 5.7. It shows that the increase of the support thickness causes an increase in weight due to the increase in the amount of material. In addition, the increase of support length does not affect the weight of geometry.

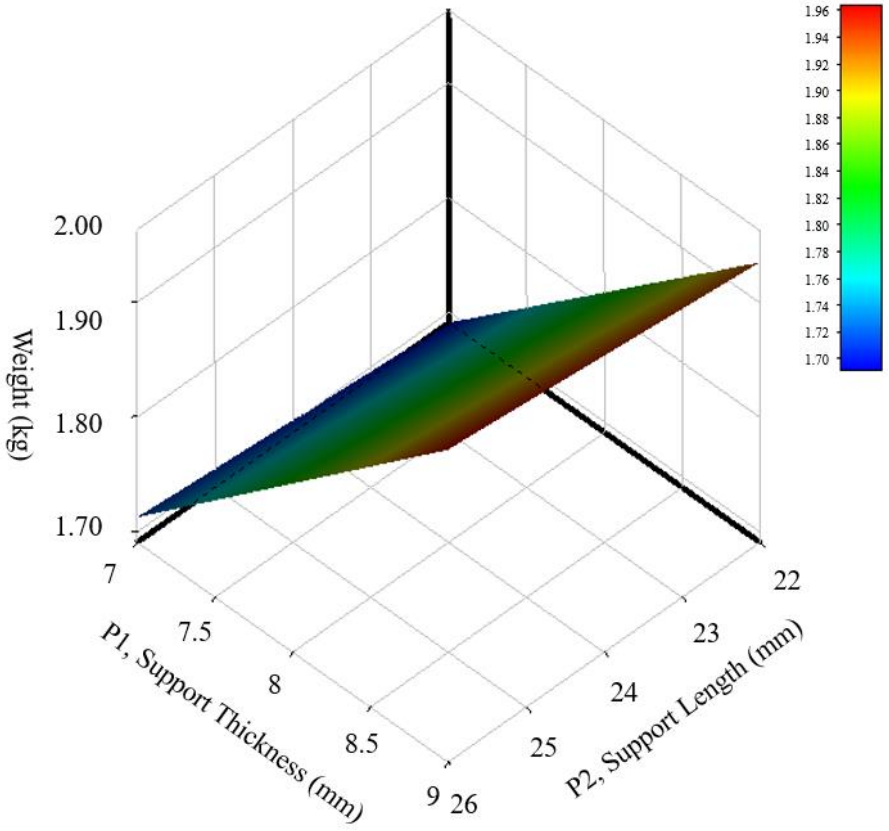

Figure 5.7. Response surface charts for the weight of geometry

Moreover, the response surface results of input parameters were also summarized in Figure 5.8 in order to observe how the geometric parameters affect. As observed from the sensitivity analysis, it can be easily seen that the support length among the input parameters has the highest effect on the output responses. However, there is no effect on the output responses for the radius of the fillet.

There is a minimal effect on the support length in the all output responses and changes depending on the output paramateres.

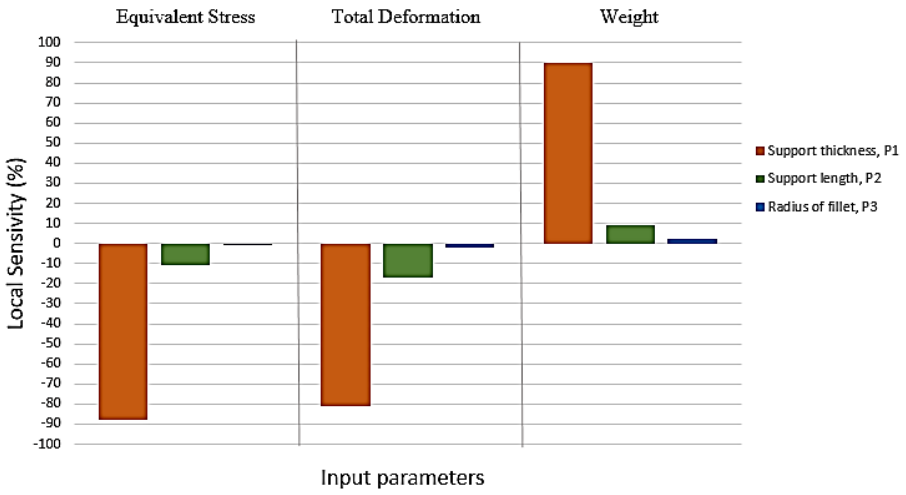

Figure 5.8. Effects of input parameters on sensitivity analysis

As a result of shape optimization with DOE shown in Table 5.2, the tenth design point among the combinations of design variables has been selected to obtain optimal design. Because, NVH (Noise, Vibration, and Harshness) problem in brake system design is one of the major issues to be considered, and one of the reasons for this problem is the inability to provide sufficient stiffness. For that reason, in order to eliminate the NVH problem, total deformation should keep as minimum as possible by satisfying the lightweight structure.

Table 5.3. Determined optimum dimensions of final design

Support thickness, P1	8.9 mm
Support length, P2	24.0 mm
Radius of fillet, P3	10.8 mm
Total weight	1.94 kg
Maximum equivalent stress	225 MPa
Maximum total deformation	0.59 mm

Consequently, support thickness (P1) is defined as 8.9 mm, support length (P2), 24 and radius of fillet (P3), 10.8. In addition, the maximum equivalent stress and the maximum total deformation on the structure are obtained as 225 MPa and 0.59 mm, respectively and the total weight is calculated as 1.95 kg.

The final design as a result of the shape optimization study is obtained as shown in Figure 5.9. Table 5.4. presents the weight comparison of the existing and optimized shaft bracket.

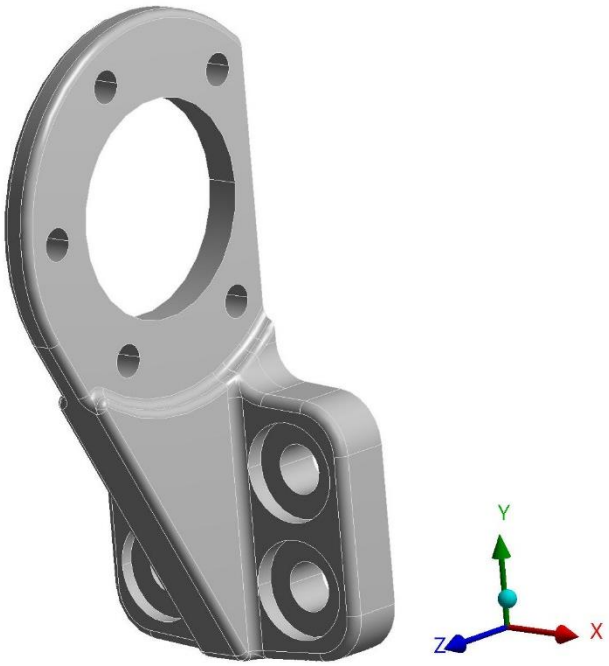

Figure 5.9. Optimized final design

Table 5.4. Weight comparison of existing and optimized shaft bracket

Existing shaft bracket	7 kg
Optimized final design	1.95 kg
Change	72%

5.2. Finite Element Analysis of Final Design

Reliability of structural integrity of the shaft bracket with optimum dimensions obtained from shape optimization according to the OSFD, new CAD model must be verified by using FEA. Here, in ANSYS® 2019 R3 environment, the boundary conditions and mesh parameters were used the same as in Section 3.2. Furthermore, in addition to FEM indicated in Section 4.1.3, bolts and vehicle axle part were included in the analysis taking into account the real working conditions of the shaft bracket in simplied manner. The illustration of the finite element model is shown in Figure 5.10.

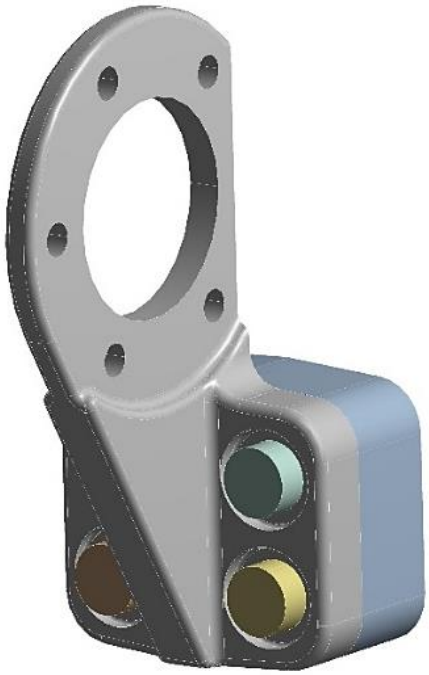

Figure 5.10. Finite element model of the final design

FEA is conducted according to the 15 kN air chamber force under static structural loading conditions. Boundary conditions, reaction force, and bolt pretensions are modeled. The material properties were multi-linear for GGG50 used in the bracket, bi-linear 10.9 steel used in bolts, and linear steel used for dummy mounting part. Chamber force 15 kN is applied on the inner surface of the bushing mounting region. Contact definition is defined automatically in ANSYS®. However, since these contact definitions

are made according to default settings, they cannot accurately simulate the analysis to be performed. Therefore, default contacts need to be redefined. Here, a part with a simplified design is used to simulate the vehicle axle and it has four holes to mount the shaft bracket to the vehicle axle. This simplified axle part is fixed on all surfaces to exhibit rigid behavior. Since there is a relative sliding motion between the shaft bracket mounting surface and the simplified vehicle axle part, frictional contact is defined as 0.3. The bolts are fixed to the mounting holes on the simplified vehicle axle part by applying bonded contact and frictional contact is defined between the surfaces of the heads of the bolts and the contact surface of the shaft bracket as 0.2. In addition, bolt pretension is applied to examine the stress created by bolt preload on the part.

The bolts to be used for assembly to the vehicle axle are determined in accordance with ISO 15071 standard and bolt pretensions are applied regarding the DIN 13 standard. The mechanical properties of the bolt are given in Table 5.5.

Table 5.5. Mechanical properties of bolt

Nominal size	14 mm
Quality	10.9
Bolt pretension	79846 N
Tightening torque	154 Nm

Boundary conditions for the final design to be used in FEA is shown in Figure 5.10.

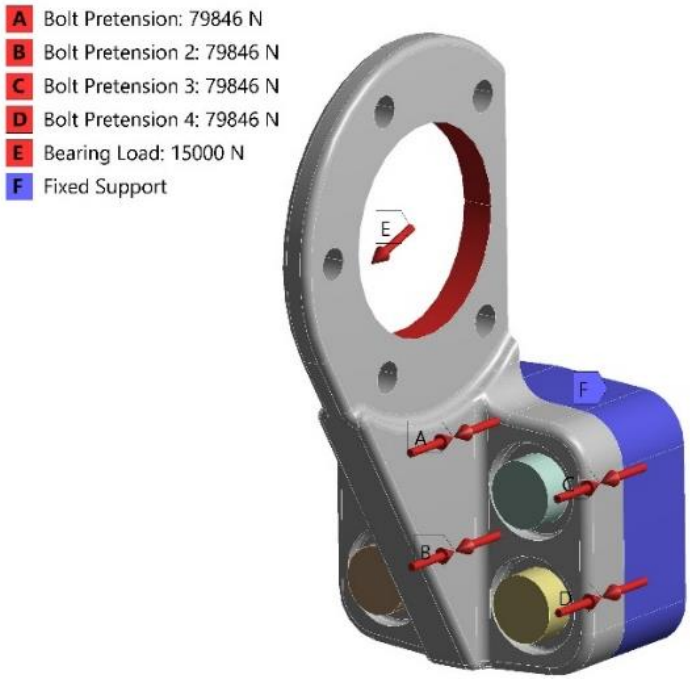

Figure 5.11. Boundary conditions of the final design

FEA results of the final shaft bracket design obtained after the shape optimization were presented in Figures 5.12-13. According to the performed FEA results, the design requirements of the shaft bracket were satisfied for the defined boundary condition.

As seen in Figure 5.12, as a result of the FEA for the final design, the maximum equivalent stress value on the shaft bracket is 225.43 MPa. Therefore, it can be seen that the maximum stress occurred is in the bushing mounting surface of the shaft bracket and since this value is considerably lower than the yield strength value of the material, it can be concluded that the shaft bracket is statically safe under these loading conditions.

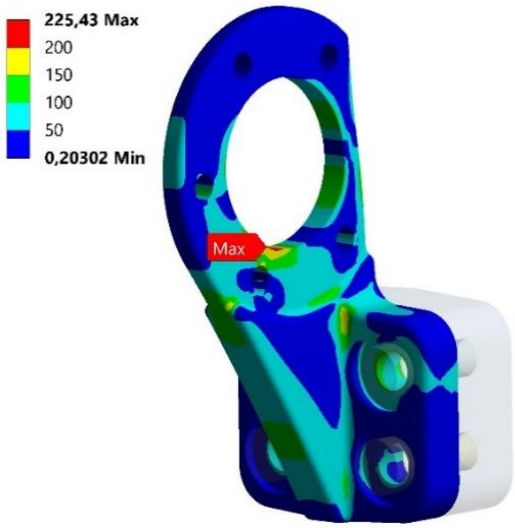

Figure 5.12. Equivalent stress distribution of the final design

As seen in Figure 5.13, the maximum total deformation value on the shaft bracket is 0.59 mm. This value is considered acceptable because it will not negatively affect brake operation and will not cause interference between brake components. However, this value should be investigated experimentally in terms of NVH problems that may occur on the vehicle.

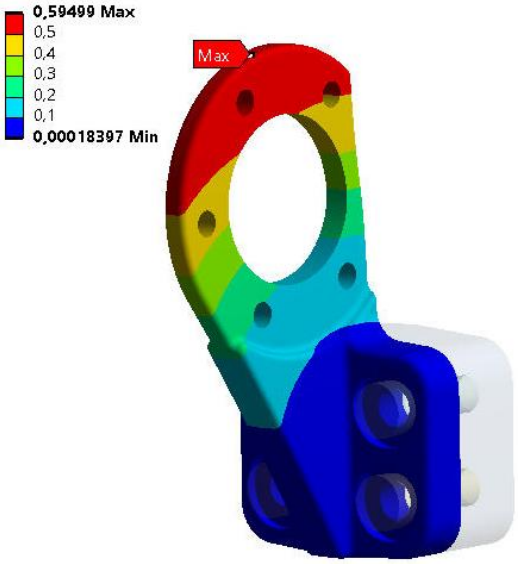

Figure 5.13. Total deformation of the final design

CHAPTER 6

EXPERIMENTAL VALIDATION

The shaft bracket is one of the essential components of the brake system. In case of emergency braking, components of the brake system must have high mechanical strength subjected to a large load. In this sense, a new shaft bracket design instead of the existing shaft bracket was obtained with the help of the optimization method and verified with FEA. However, in order to verify the reliability, maintainability and performance of the optimization methods, an experimental validation test is performed simulating the same working condition. Here, the prototype of the shaft bracket was manufactured from GGG50 material with the traditional casting method according to the optimal dimensions shown in Table 5.3, as a result of the optimization. The prototype of the shaft bracket is shown in Figure 6.1.

Figure 6.1. Casted and machined prototype of shaft bracket

After the casting and machining process, an experimental validation test was set up to perform the durability of the structure and verify the result obtained from FEA. The experimental test consisted of some components such as vehicle axle, Z-cam brake, air brake chamber, shaft bracket, brake drum, datalogger. In this sense, firstly, the shaft bracket was mounted on the vehicle axle with fixation bolts. And then, other related components such as air brake chamber, bushing, etc. were assembled to the test rig. Furthermore, the datalogger system was connected to capture related data such as stress, and air pressure. The experimental test rig is shown in Figure 6.2.

Figure 6.2. The experimental validation test rig

After completing the assembly process, a strain gauge was mounted on a suitable surface of the shaft bracket in order to measure the stress more accurately. For that reason,

the strain gauge was placed near the fixation hole shown in Figure 6.2 according to the stress result in section 5.2.

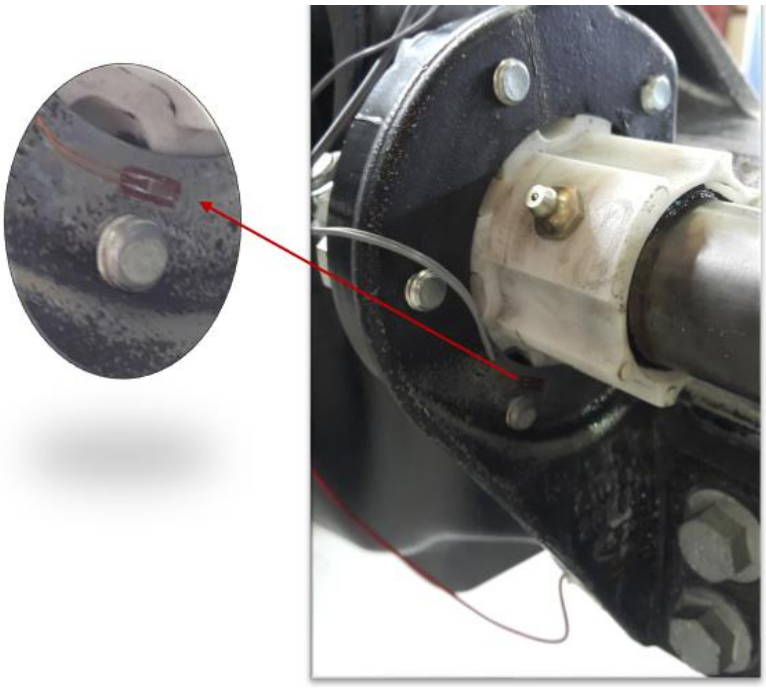

Figure 6.3. Strain gauge application for shaft bracket

The measurement was conducted for a minimum of 10 braking applications. Here, the signal obtained from strain gauge was processed by the datalogger and plotted together with stress based on the orange line and pressure based on the blue line. As a result of the measurement, the average stress was measured approximately 165 MPa and this result compared with the equivalent stress distribution of the final model FEA in section 5.2. The stress measurement resulting from the test is shown in Figure 6.4 and the

detailed FEA result is shown in Figure 6.5. Thus, it can be said that the experimental test provides a considerable correlation compared with FEA.

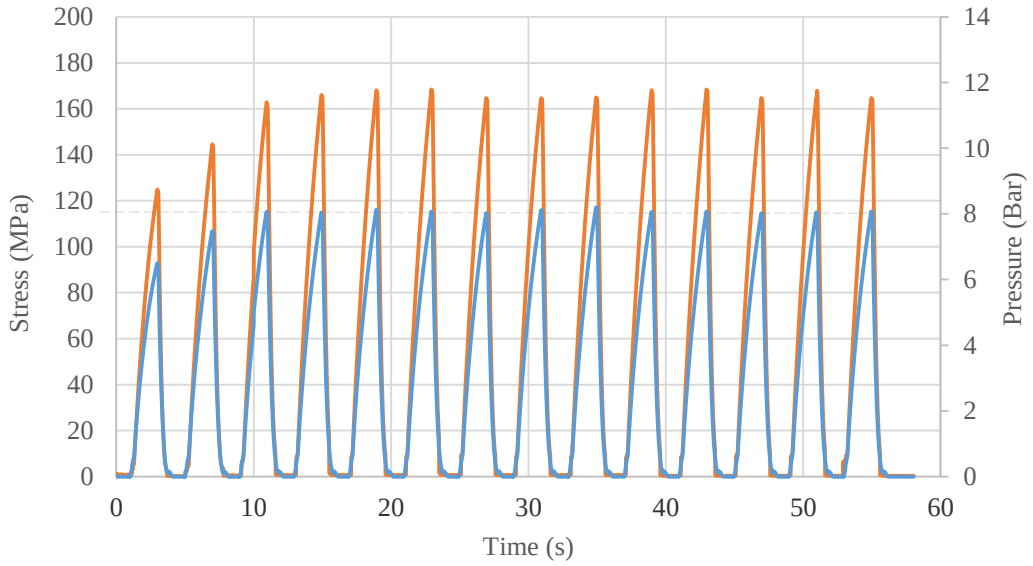

Figure 6.4. Test result of strain gauge application

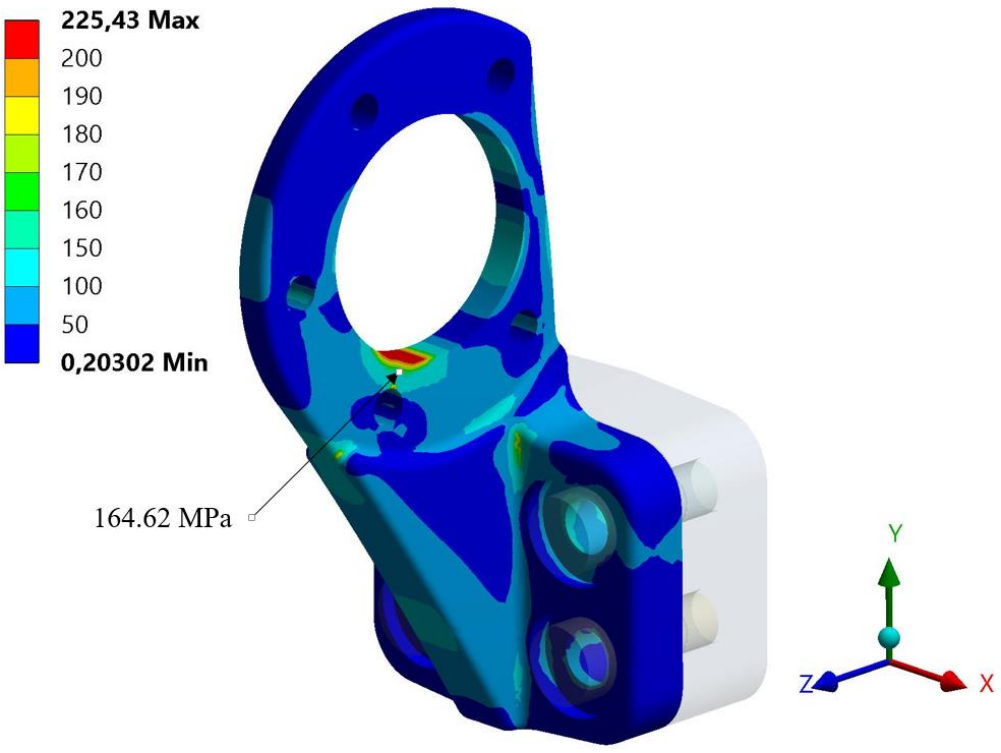

Figure 6.5. Equivalent stress distribution at strain gauge location

After stress measurement is done successfully, a fatigue test is performed for the manufactured prototype of the shaft bracket. Fatigue is the weakening of a material caused by repeatedly applied loads. Estimating the failure time distribution or long-term performance of components of high-reliability products is particularly difficult. Most structures are designed to operate without failure within targeted life. However, fatigue occurs when a material is subjected to cyclic loading. If the loads are above a certain threshold, microscopic cracks will form at the stress concentrators. Eventually, these cracks will reach critical size suddenly and the structure will fracture.

In the fatigue test, 15 kN air brake chamber force is applied as brake force to generate the specified brake torque around 8 bar pressure and this test is performed for 100000 braking applications.

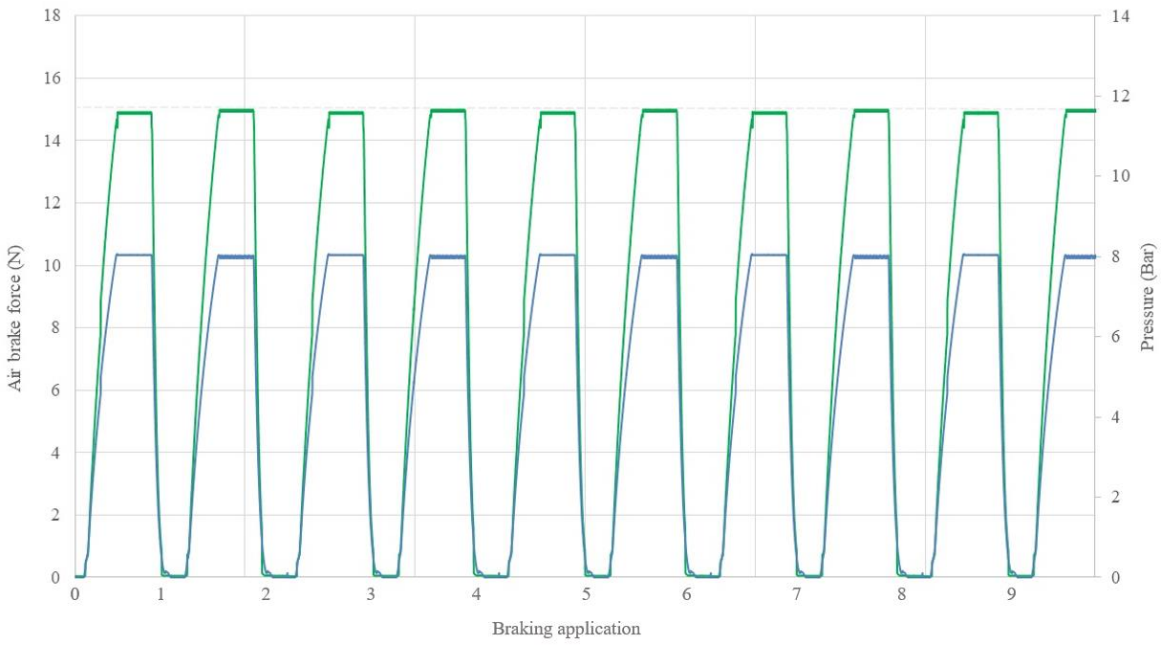

Figure 6.6. Fatigue test result

As a result of the experimental validation test, it was determined that the shaft bracket preserved its functionality and durability. Furthermore, permanent deformation, cracks and fractures were not detected as a result of non-destructive inspections of the shaft brackets.

CHAPTER 7

CONCLUSION

This thesis aimed to achieve an optimal design instead of the existing shaft bracket which is used in Z-cam drum brakes of heavy duty vehicles with the help of optimization methods. First, a suitable three-dimensional design space in accordance with the vehicle axle platform was created via CAD software, SolidWorks® 2018. Then, the reaction forces acting on the shaft bracket were calculated by kinematic analysis of Z-cam drum brake free body diagram and FEM was built with ANSYS® under the determined boundary conditions. Furthermore, FE combined topology optimization was performed using the SIMP algorithm. Here, mass minimization under stress constraint was conducted. As a result of topology optimization, the rough material distribution of the structure was obtained, and then shape optimization by RSM was conducted to obtain the final geometry. Three critical design parameters were identified based on manufacturability and response surfaces were created for weight, stress, and total deformation using the OSFD method. Thus, optimum dimensions of the final design were determined to remain within the acceptable stress limit. FEA of the final design was repeated to ensure whether mechanical strength and stiffness of structure were satisfied for the same boundary conditions. Finally, the prototype produced from GGG50 material for the new shaft bracket design obtained after the optimization processes were performed to experimental validation tests at EGE FREN SAN. TİC. A.Ş.

As a result of the study, by comparing the validated test results with FEA results, the capability and applicability of the optimization method used in the product design were examined. According to the results, the optimization methods provided remarkably reduced weight up to 72% compared to the existing shaft bracket within the acceptable stress limit. The density-based topology optimization with mass minimization provided a significant product layout solution to create the lightweight design. The RSM using OSFD was also an effective shape optimization method within limited design resources satisfying all design requirements under determined boundary conditions. In addition, the FEA result of the final design provided a good correlation with experimental test results

and experimental tests results proved that the final design obtained by optimization methods performed similar structural performance compared to the existing shaft bracket. Consequently, the structural optimization methods comprising topology and response surface optimization combination indicated powerful and cost-effective product design solutions to be possible to design light-weight, high-performance vehicle products in a shorter time without prior knowledge about product layout.

REFERENCES

Abdi, M. 2015. Evolutionary Topology Optimization Of Continuum Structures Using X-FEM and İsovalues Of Structural Performance (Doctoral dissertation, University of Nottingham).

Albak, E. İ. 2019. Formula SAE Aracında Ağırlık Azaltılmasına Yönelik Fren Pedalının Topoloji Optimizasyonu Yöntemiyle Optimum Tasarımı. *Uluslararası Mühendislik Araştırma ve Geliştirme Dergisi*, 11(1), p. 328-334.

Ansys, I. 2013. ANSYS Meshing User's Guide, Ansys.

Ansys, Inc. 2019. *ANSYS Release Notes Reference*, Release 2019 R3.

Arora, J. S. 2004. Introduction to Optimum Design. *Elsevier*.

Awate, S. B., Bajaj, R. V. & Bhosale, A., 2016. Experimental Validation & Testing of Brake Chamber Mounting Bracket, *International Research Journal of Engineering and Technology*, 3(6), p. 3001-3005.

Baba, S. N. N., Hamid, M. N. A., Soid, S. N. M., Zahelem, M. N., & Omar, M. S. 2018. Analysis of Drum Brake System for Improvement of Braking Performance. *In Engineering Applications for New Materials and Technologies*, p. 345-357.

Bendsøe, M. P. 1989) Optimal Shape Design As A Material Distribution Problem. *Structural optimization*, 1(4), p. 193-202.

DIN 74060-1:1992. Air Braking Systems; Pneumatic Actuator; Brake Chamber; Technical Data, DIN Deutsches Institut für Normung, Berlin, Germany.

Doğan, O. 2015. Yeni Nesil Traktörler İçin Yüksek Tork Aktarımına Sahip Uzun Ömürlü Debriyaj Tasarımı (Master's thesis, Uludağ Üniversitesi).

Düzcan, Y. 2019. Yapısal Optimizasyon Teknikleri İle Taşıt Süspansiyon Bileşenlerinin Geliştirilmesi (Master's thesis, Bursa Uludağ Üniversitesi).

Enginar, H. E. 2014. Ağır Taşıt Jantının Topoloji Optimizasyonu Yardımıyla Optimum Tasarımı (Master's thesis, Dokuz Eylül Üniversitesi).

Erten, H. I., Deveci, H. A. & Artem, H. S. 2020. Stochastic Optimization Methods p. 10-23. CRC Press.

Fornace, L. V. 2006. Weight Reduction Techniques Applied to Formula SAE Vehicle Design: An Investigation in Topology Optimization (Doctoral dissertation, University of California).

Ghazaly, N. M., & Mostafa, M. M. 2014. Experimental Investigation of Drum Brake Performance for Passenger Car. *In Proceedings of The IIER-Science Plus International Conference,* Kuala Lumpur Malaysia, 18th October.

Grinde, S., 2018. Topology Optimization For Additive Manufacturing Using SIMP Method (Bachelor's thesis, Montana Tech).

Güleryüz, İ. C. 2019. Lightweight Design of A Torque Plate of Z-Cam Drum Brake For Heavy Duty Vehicles. *International Journal of Automotive Science and Technology*, 3(2), p. 42-50.

ISO 15071: 2011. Hexagon Bolts With Flange Small Series Product Grade A, *ISO International Organization for Standardization*, Geneva, Switzerland.

Işık, E. 2009. Topoloji Optimizasyonu: Çatallı Flanş Uygulaması (Doctoral dissertation, DEÜ Fen Bilimleri Enstitüsü).

İpek, S. 2011. Doğru Mesh Üretiminin Çözüm Üzerindeki Etkileri (Master's thesis, Isparta Üniversitesi).

Jensen, F. 2018. Topology Optimization of Turbine Manifold in the Rocket Engine Demonstrator Prometheus Master's thesis, Luleå University of Technology).

Keten, A. 2020. Direksiyon Mafsalının Yapısal Optimizasyon Yöntemleri İle Hafifliğinin Sağlanması (Master's thesis, Uludağ Üniversitesi).

Kumar, P. 2017. Synthesis of Large Deformable Contact-Aided Compliant Mechanisms Using Hexagonal Cells and Negative Circular Masks (Doctoral dissertation, , Indian Institute of Technology Kanpur).

Kuralay, N. S., & Taşıtlar, M. 2008. Temel ve Tasarım Esasları. *Yapı Elemanları, Izmir: TMMOB Makina Mühendisleri Odası.*

Kuram, E., Ozcelik, B., Bayramoglu, M., Demirbas, E., & Simsek, B. T. 2013. Optimization of Cutting FluidsaAnd Cutting Parameters During End Milling by Using D-Optimal Design of Experiments. *Journal of Cleaner Production,* 42, p. 159-166.

Limpert, R. 2011. Brake Design and Safety (pp. i-xv). *SAE*.

Li, X. & Wang, L. 2012. Based on Topology Optimization Method the Cab Mount Bracket Lightweight Design. *In Applied Mechanics and Materials*, 152, p. 1292-1297).

Liu, S., Li, Q., Liu, J., Chen, W., & Zhang, Y. 2018. A Realization Method for Transforming A Topology Optimization Design Into Additive Manufacturing Structures. *Engineering*, 4(2), p. 277-285.

Mahmoud, K. R. M. 2005. Theoretical and Experimental İnvestigations on A New Adaptive Duo Servo Drum Brake With High and Constant Brake Shoe Factor. *HNI*.

Mathur, A., & Kurna, S. 2015. Weight Optimization of Axle Beam Using Optistruct. *In Altair Technology Conference*, India.

Menon, A. 2005. Structural Optimization Using Ansys and Regulated Multiquadric Response Surface Model. (Master's thesis, The University of Texas at Arlington).

Mlejnek, H. P. & Schirrmacher, R. 1993. An Engineer's Approach to Optimal Material Distribution and Shape Finding. *Computer methods in applied mechanics and engineering*, 106(1-2), p. 1-26.

Mutlu, F. & Kayacan, M. C. 2019. Bir Düz Dişlinin Eklemeli İmalata Göre Topoloji Optimizasyonunun Araştırılması, *4th International Congress on 3D Printing (Additive Manufacturing) Technologies And Digital Industry*, p. 1196-1204.

Nagatani, H., & Niwa, T. 2005. Application of Topology Optimization and Shape Optimization for Development of Hub-bearing Lightening, *NTN Technical Review*, 73, p. 14-19.

Olason, A., & Tidman, D. 2010. Methodology for Topology and Shpe Optimization In The Design Process.

Özçelik, M. 2011. Taşıt Askı Sistemi Elemanlarının Farklı Yol Koşulları İçin Parametrik Kütle Optimizasyonu (Master's thesis, Dokuz Eylül Üniversitesi).

Quincha Munoz, J. S. 2017. Engineering Optimization Showcase (Doctoral dissertation, University of Queensland).

Qadeer, M. 2018. Experimental Validation of Topology Optimization and Lattice Design For Additive Manufacturing of a Polymeric Bracket (Doctoral dissertation, Politecnico di Torino).

Rao, S. S. 2019. Engineering Optimization: Theory and Practice. John Wiley & Sons.

Ren, M. Y. & Vipradas, A. 2021. ANSYS DOE and Design Optimization Tutorial. *School for Engineering of Matter, Transport and Energy. Arizona: Arizona State University.*

Salem, N. 2017. Parameterized Finite Element Analysis With Optimization of a Superplastic Forming Process Using Ansys®. *DAAAM International Scientific Book*, p. 319-332

Sant'Anna, H. M., & Fonseca, J. S. 2002. Topology Optimization of Continuum Two-Dimensional Structures Under Compliance And Stress Constraints. *Mecanica Computacional*, 1, p. 2732-2751.

Sergent, N., Tirovic, M., & Voveris, J. 2014. Design Optimization of an Opposed Piston Brake Caliper. *Engineering Optimization*, 46(11), p. 1520-1537.

Sudin, M. N., Tahir, M. M., Ramli, F. R., & Shamsuddin, S. A. 2014. Topology Optimization in Automotive Brake Pedal Redesign. *International Journal of Engineering and Technology.* 6(1): p. 398-402.

Thummar, D. R. 2014. Truss Topology Optimization Using Modified Genetic Algorithm. *Master of Technology in Machine Design*, Department of Mechanical Engineering School of Engineering, RK University, Rajkot, Gujarat-360020.

Topac, M. M., & Atak, M. 2016. Optimal Design of A Rigid Front Axle Beam For Trucks. *In 1st International Mediterranean Science and Engineering Congress (IMSEC 2016)*, Çukurova University, Congress Center, Adana/Turkey.

Topac, M. M., Karaca, M., Aksoy, B., DERYAL, U., & Bilal, L. 2020. Lightweight Design of A Rear Axle Connection Bracket for A Heavy Commercial Vehicle By Using Topology Optimisation: A Case Study. *Mechanics*, 26(1), p. 64-72.

Tyflopoulos, E., Tollnes, F. D., Steinert, M., & Olsen, A. 2018. State of the Art of Generative Design and Topology Optimization and Potential Research Needs, *DS 91: Proceedings of NordDesign 2018*, Linköping, Sweden.

Tyflopoulos, E., & Steinert, M. 2020. Topology and Parametric Optimization-Based Design Processes for Lightweight Structures. *Applied Sciences*, 10(13), 4496.

Verbart, A. 2015. Topology Optimization With Stress Constraints (Doctoral dissertation, National Aerospace Laboratory).

Willis, R., & Finney, B. A. 2012. Environmental Systems Engineering and Economics. *Springer Science & Business Media*.

Yaban, E. 2012. Bir Uçağın Basınç Duvarının Yapısal Optimizasyonu (Master's thesis, Gazi Üniversitesi).

Yalamanchili, V. K. & Kumar, A. V. 2012. Topology Optimization of Structures Using A Global Stress Measure. *In International Design Engineering Technical Conferences and Computers and Information in Engineering Conference,* 45011, p. 1321-1328).

Yıldız, A. R., Kaya, N., Öztürk, F., & Alankus, O. 2004. Optimal Design of Vehicle Components Using Topology Design and Optimisation. *International Journal of Vehicle Design*. 34(4): p. 387-398.

Zhang, J. D., Zheng, B., & Lai, D. 2019. Finite Element Analysis and Optimization of Brake Shoe of Drum Brake. *In 2019 IEEE 3rd Information Technology, Networking, Electronic and Automation Control Conference (ITNEC).* p. 2381-2385.

Zhou, M. & Rozvany, G. 1991. The Coc Algorithm, Part ii: Topological, Geometrical and Generalized Shape Optimization. *Computer Methods in Applied Mechanics and Engineering*, 89(1), p. 309-336.